Computational Mechanics 33 (2004) 435–452 © Springer-Verlag 2004
DOI 10.1007/s00466-003-0544-y

A complete finite element treatment for the fully coupled implicit ALE formulation

H. N. Bayoumi, M. S. Gadala

Abstract This paper presents a complete derivation and implementation of the Arbitrary Lagrangian Eulerian (ALE) formulation for the simulation of large deformation quasi-static and dynamic problems. While most of the previous work done on ALE for dynamic applications was mainly based on operator split and explicit calculations, this work derives the quasi-static and dynamic ALE equations using a fully coupled implicit approach. Full expression for the ALE virtual work equations and finite element matrices are given. Time integration relations for the dynamic equations are also derived. Several quasi-static and dynamic large deformation applications are solved and presented.

Keywords Finite element analysis, Arbitrary lagrangian eulerian formulation, ALE, Large deformation, Mesh motion, Coupled formulations, Implicit dynamic analysis

1 Introduction

The Arbitrary Lagrangian Eulerian (ALE) formulation has emerged in recent years as a technique that can alleviate many of the drawbacks of the traditional Lagrangian and Eulerian formulations [2, 5, 7, 11, 16]. Using ALE, the computational grid need not adhere to the material nor be fixed in space but can be moved arbitrarily. The grid is continuously moved to optimize element shapes independently from material deformation. A proper ALE formulation should reduce to both the Lagrangian and Eulerian formulations at any degree of freedom as desired. Combining the merits of both the Lagrangian and Eulerian formulations, ALE can easily describe different types of boundary conditions and prevent mesh distortion.

The ALE equations are derived by substituting the relationship between the material time derivative and grid time derivative into the continuum mechanics governing equations. This substitution gives rise to convective terms in the ALE equations which account for the transport of material through the grid. ALE is usually termed a coupled formulation since material deformation and convective effects are coupled in the same equations. A survey of the ALE literature [17], however, shows that the majority of ALE analyses, whether quasi-static or dynamic, are based on the computationally convenient operator split technique. In this approach, material deformation and convective effects are treated separately. Thus each time step may be divided into two steps: a regular Lagrangian step followed by an Eulerian step. The main advantage of this technique over the fully coupled approach is the reduction in the cost of implementation of ALE to current Lagrangian codes as the Lagrangian step is unchanged and only the Eulerian step algorithm needs to be added. Moreover, the decoupling of the Lagrangian and Eulerian steps results in simpler equations to be solved. However, from the theoretical point of view, the fully coupled ALE approach represents a true kinematic description in which material deformation is described relative to a moving reference configuration.

In this work, a complete treatment for the fully coupled implicit ALE formulation is presented. Virtual work equations are first derived from the basic principles of continuum mechanics. Next, finite element descritization of the virtual work equations is performed. Full expression for the resulting finite element matrices and vectors are also given. A method for condensing out grid displacements and processing of the equivalent stiffness matrix on the element level is presented. Finally, several quasi-static and dynamic large deformation applications are solved and discussed.

2 Basic ALE equations

2.1 Notations

The governing ALE equilibrium equations will be derived for use with an implicit time-stepping approach. In this approach, we assume that the solution for the equilibrium positions at all time steps from time 0 to time t have been solved for, and that the solution for time $t + \Delta t$ is required next. Throughout this paper, standard indicial notations are adopted; right subscripts denote the components of a tensor and repeated subscripts imply summation. In addition, time and configuration notations similar to those used by Bathe [1] are adopted. Left superscripts indicate the configuration in which the quantity occurs whereas left subscripts indicate the configuration to which the quantity is referred. Left

Received: 3 April 2003 / Accepted: 4 December 2003
Published online: 13 April 2004

H. N. Bayoumi
MSC Software, 500 Arguello St #200,
Redwood City, CA 94063, USA

M. S. Gadala (✉)
University of British Columbia,
Department of Mechanical Engineering,
2324 Main Mall, Vancouver, BC, Canada V6T 2G9
e-mail: gadala@mech.ubc.ca

subscripts may be omitted if the quantity occurs in the same configuration in which it is measured. A quantity with no left superscripts or subscripts indicate an incremental quantity from time t to $t + \Delta t$.

2.2 Kinematics

In the ALE description, the material configuration at any time t refers to the set of material particles, whereas the reference configuration consists of a set of arbitrarily moving grid points sharing a common boundary with the set of material particles. The material configuration is identified by a set of material point coordinates X_i^m while the reference, or grid, configuration is identified by an independent set of grid point coordinates X_i^g. Let ${}^t x_i^m(X_j^m, t)$ and ${}^t x_i^g(X_j^g, t)$ be the vector functions or the mappings that characterize the motion of the material point X_j^m and the grid point X_j^g in space, respectively. The position of X_j^m at time t is given by

$$ {}^t x_i = {}^t x_i^m(X_j^m, t) \tag{1} $$

The set of material particles is related to the set of grid points by requiring that the two configurations share the same space at all times. Any point within the common boundary is occupied by elements of the two sets. Thus, the position of the grid point X_j^g that occupies the same point in space at time t as X_j^m is also given by ${}^t x_i$ as

$$ {}^t x_i = {}^t x_i^g(X_j^g, t) \tag{2} $$

The ALE formulation requires that the inverse of (1) and (2) exist to ensure a one-to-one mapping between the two configurations. The material velocity ${}^t v_i$ and the grid point velocity ${}^t v_i^g$ at time t are given by

$$ {}^t v_i = \left. \frac{\partial^t x_i^m}{\partial t} \right|_{X_j^m} \tag{3} $$

$$ {}^t v_i^g = \left. \frac{\partial^t x_i^g}{\partial t} \right|_{X_j^g} \tag{4} $$

The boundary constraint, which ensures that the material and grid configurations have the same boundary at all times, can be expressed in the form

$$ ({}^t v_i - {}^t v_i^g) {}^t n_i \big|_{\text{on the boundary}} = 0 \tag{5} $$

where ${}^t n_i$ is the unit normal to the boundary surface.

The governing ALE equations involve the material time derivative of several quantities. The material derivative of an arbitrary function ${}^t f$ is denoted by a superposed dot and is defined to be the rate of change of the function holding the material particle X_i^m fixed

$$ {}^t \dot{f} = \left. \frac{\partial^t f}{\partial t} \right|_{X_i^m} \tag{6} $$

However, the grid configuration is the computational configuration that tracks the history of all quantities. Thus, it is convenient to define a grid time derivative, which is the time derivative of the function ${}^t f$ holding the grid point X_i^g fixed, and denote it by a superposed prime

$$ {}^t f' = \left. \frac{\partial^t f}{\partial t} \right|_{X_i^g} \tag{7} $$

The relation between the two time derivatives is given by [9]

$$ {}^t \dot{f} = {}^t f' + ({}^t v_i - {}^t v_i^g) \frac{\partial^t f}{\partial^t x_i} \tag{8} $$

Employing displacement based finite elements, we denote the incremental material displacements from time t to time $t + \Delta t$ by u_i and the corresponding incremental grid displacements by u_i^g. We have the following relation

$$ {}^{t+\Delta t} x_i = {}^t x_i + u_i^g \tag{9} $$

where ${}^{t+\Delta t} x_i$ is the position of the grid point in the configuration at time $t + \Delta t$.

2.3 Continuity

The local form of conservation of mass, continuity, at time t is given by

$$ {}^t \dot{\rho} = -{}^t \rho \frac{\partial^t v_i}{\partial^t x_i} \tag{10} $$

where ${}^t \rho$ is the material density. Using (8), the continuity equation with respect to an arbitrary moving grid point can be expressed as

$$ {}^t \rho' = -{}^t \rho \frac{\partial^t v_i}{\partial^t x_i} - ({}^t v_i - {}^t v_i^g) \frac{\partial^t \rho}{\partial^t x_i} \tag{11} $$

3 Quasi-static analysis

3.1 Principle of virtual displacements

For quasi-static analysis, as in the case of low-speed metal forming processes, inertia effects may be neglected. Employing an implicit incremental approach, the governing equilibrium equations for ALE are established for the configuration of the body at time $t + \Delta t$. Since the configuration at time $t + \Delta t$ is yet unknown, an approximate solution is usually obtained by referring all variables to the grid configuration at time t and linearizing the resulting equations. The solution is then refined by iterations.

The principle of virtual displacements is employed to express the equilibrium of the body at time $t + \Delta t$. It can be written in the form

$$ \int_{{}^{t+\Delta t}V} {}^{t+\Delta t}\sigma_{ij} \delta_{t+\Delta t} e_{ij} \, {}^{t+\Delta t} \mathrm{d}V = \delta^{t+\Delta t} W^{ext} \tag{12} $$

where ${}^{t+\Delta t}\sigma_{ij}$ are the components of the true (or Cauchy) stress tensor at time $t + \Delta t$ and ${}_{t+\Delta t}e_{ij}$ is the work conjugate true strain tensor defined by

$$ {}_{t+\Delta t}\mathrm{e}_{ij} = \frac{1}{2} \left(\frac{\partial u_i}{\partial^{t+\Delta t} x_j} + \frac{\partial u_j}{\partial^{t+\Delta t} x_i} \right) \tag{13} $$

The external virtual work, $\delta^{t+\Delta t} W^{ext}$, is given by

$$\delta^{t+\Delta t}W^{\text{ext}} = \int_{t+\Delta t V} {}^{t+\Delta t}\rho^{t+\Delta t} f_i^B \delta u_i^{t+\Delta t} \mathrm{d}V + \int_{t+\Delta t S} {}^{t+\Delta t} f_i^S \delta u_i^{t+\Delta t} \mathrm{d}S \tag{14}$$

in which ${}^{t+\Delta t}f_i^B$ and ${}^{t+\Delta t}f_i^S$ are the components of the body force per unit mass and the surface traction at time $t+\Delta t$, respectively.

3.2 Incremental decompositions

In referring variables to the grid configuration, variables at time $t+\Delta t$ are assumed to be composed of their respective values at time t plus an increment given by the grid time derivative of the variable multiplied by the time increment Δt.

Material density at time $t+\Delta t$ can be decomposed into

$${}^{t+\Delta t}\rho = {}^{t}\rho + {}^{t}\rho' \Delta t \tag{15}$$

which, upon substituting (11), gives

$${}^{t+\Delta t}\rho = {}^{t}\rho - {}^{t}\rho \frac{\partial u_k}{\partial^t x_k} - (u_k - u_k^g)\frac{\partial^t \rho}{\partial^t x_k} \tag{16}$$

Stress components at time $t+\Delta t$ can be expressed in terms of the stresses at time t for the same grid point plus a stress increment ${}^{t}\sigma'_{ij}\Delta$t

$${}^{t+\Delta t}\sigma_{ij} = {}^{t}\sigma_{ij} + {}^{t}\sigma'_{ij}\Delta t \tag{17}$$

and using (8), we get

$${}^{t+\Delta t}\sigma_{ij} = {}^{t}\sigma_{ij} + {}^{t}\dot{\sigma}_{ij}\Delta t - (u_k - u_k^{\mathrm{g}})\frac{\partial^t \sigma_{ij}}{\partial^t x_k} \tag{18}$$

The material rate of Cauchy stresses ${}^{t}\dot{\sigma}_{ij}$ is calculated from the material constitutive relation which is usually given in terms of an objective stress rate tensor such as the Truesdell stress rate tensor defined by

$${}^{t}\sigma_{ij}^{\mathrm{T}} = {}^{t}\dot{\sigma}_{ij} + \frac{\partial^t v_k}{\partial^t x_k}{}^{t}\sigma_{ij} - \frac{\partial^t v_j}{\partial^t x_k}{}^{t}\sigma_{ik} - \frac{\partial^t v_i}{\partial^t x_k}{}^{t}\sigma_{jk} \tag{19}$$

Restricting the analysis to elastic-plastic materials, the material constitutive relation in terms of the Truesdell stress rate is given by

$${}^{t}\sigma_{ij}^{\mathrm{T}} = {}^{t}C_{ijkl}^{\mathrm{EP}}\,{}^{t}D_{kl} \tag{20}$$

where ${}^{t}D_{ij}$ is the rate of deformation tensor given by

$${}^{t}D_{ij} = \frac{1}{2}\left(\frac{\partial^t v_i}{\partial^t x_j} + \frac{\partial^t v_j}{\partial^t x_i}\right) \tag{21}$$

and ${}^{t}C_{ijkl}^{\mathrm{EP}}$ is the fourth order elastic-plastic material constitutive tensor whose construction is presented in a later section in this work. The variation in the strain components at time $t+\Delta t$ can be decomposed as

$$\delta_{t+\Delta t}\mathrm{e}_{ij} = \delta_t \mathrm{e}_{ij} + \delta_t \mathrm{e}'_{ij}\Delta t \tag{22}$$

in which $\delta_t e'_{ij}$ is the grid time derivative of $\delta_t e_{ij}$ and is given by

$$\delta_t e'_{ij} = -\frac{1}{2}\left(\frac{\partial \delta u_i}{\partial^t x_k}\frac{\partial^t v_k^g}{\partial^t x_j} + \frac{\partial \delta u_j}{\partial^t x_k}\frac{\partial^t v_k^g}{\partial^t x_i}\right) \tag{23}$$

Substitution in (22) gives

$$\delta_{t+\Delta t}\mathrm{e}_{ij} = \delta_t \mathrm{e}_{ij} - \frac{1}{2}\left(\frac{\partial \delta u_i}{\partial^t x_k}\frac{\partial u_k^g}{\partial^t x_j} + \frac{\partial \delta u_j}{\partial^t x_k}\frac{\partial u_k^g}{\partial^t x_i}\right) \tag{24}$$

Incremental decomposition of elemental volume at time $t+\Delta t$ in terms of the elemental volume at time t is given by

$${}^{t+\Delta t}\mathrm{d}V = {}^{t}dV + {}^{t}\mathrm{d}V'\Delta t = \left(1 + \frac{\partial u_k^g}{\partial^t x_k}\right){}^{t}\mathrm{d}V \tag{25}$$

Similarly, incremental decomposition of elemental surface area is given by

$$\begin{aligned}{}^{t+\Delta t}\mathrm{d}S &= {}^{t}\mathrm{d}S + {}^{t}\mathrm{d}S'\Delta t \\ &= \left[1 + \frac{\partial u_k^g}{\partial^t x_k} - \frac{1}{2}\left(\frac{\partial u_m^g}{\partial^t x_n} + \frac{\partial u_n^g}{\partial^t x_m}\right){}^{t}n_m^t n_n\right]{}^{t}\mathrm{d}S\end{aligned} \tag{26}$$

where ${}^{t}n_m$ is the unit outward normal to the surface at time t.

3.3 Linearization

Linearization is accomplished by expanding (12) using the previous incremental decompositions and neglecting higher orders in all incremental quantities. Substituting by (18), (24), and (25), the internal virtual work can be expanded, after linearization, into

$$\begin{aligned}&\int_{t+\Delta t V} {}^{t+\Delta t}\sigma_{ij}\delta_{t+\Delta t}e_{ij}^{t+\Delta t}\mathrm{d}V \\ &= \int_{{}^{t}V} {}^{t}\sigma_{ij}\delta_t e_{ij}{}^{t}\mathrm{d}V + \int_{{}^{t}V} {}^{t}\dot{\sigma}_{ij}\Delta t\delta_t e_{ij}{}^{t}\mathrm{d}V \\ &\quad + \int_{{}^{t}V} \frac{\partial u_k^g}{\partial^t x_k}{}^{t}\sigma_{ij}\delta_t e_{ij}{}^{t}\mathrm{d}V - \int_{{}^{t}V} \frac{\partial u_k^g}{\partial^t x_j}{}^{t}\sigma_{ij}\frac{\partial \delta u_i}{\partial^t x_k}{}^{t}\mathrm{d}V \\ &\quad - \int_{{}^{t}V} (u_k - u_k^g)\frac{\partial^t \sigma_{ij}}{\partial^t x_k}\delta_t e_{ij}{}^{t}\mathrm{d}V\end{aligned} \tag{27}$$

Considering the external virtual work on the RHS of (12), the body force term can be referred to the grid configuration by using (16) and (25) to get

$$\begin{aligned}&\int_{t+\Delta t V} {}^{t+\Delta t}\rho^{t+\Delta t} f_i^{\mathrm{B}} \delta u_i^{t+\Delta t}\mathrm{d}V \\ &= \int_{{}^{t}V} {}^{t}\rho^{t+\Delta t} f_i^{\mathrm{B}} \delta u_i{}^{t}\mathrm{d}V \\ &\quad - \int_{{}^{t}V} {}^{t}\rho^{t+\Delta t} f_i^{\mathrm{B}}\left(\frac{\partial u_k}{\partial^t x_k} - \frac{\partial u_k^g}{\partial^t x_k}\right)\delta u_i{}^{t}\mathrm{d}V \\ &\quad - \int_{{}^{t}V} {}^{t+\Delta t} f_i^{\mathrm{B}}(u_k - u_k^g)\frac{\partial^t \rho}{\partial^t x_k}\delta u_i{}^{t}\,\mathrm{d}V\end{aligned} \tag{28}$$

Similarly, by using (26), the traction force term of the external virtual work can be expressed as

$$\int_{t+\Delta t_S} {}^{t+\Delta t}f_i^S \delta u_i{}^{t+\Delta t}\mathrm{d}S = \int_{{}^tS} {}^{t+\Delta t}f_i^S \left[1+\frac{\partial u_k^g}{\partial {}^tx_k}-\frac{1}{2}\left(\frac{\partial u_m^g}{\partial {}^tx_n}+\frac{\partial u_n^g}{\partial {}^tx_m}\right){}^tn_m{}^tn_n\right]\delta u_i{}^t\mathrm{d}S \tag{29}$$

3.4 Treatment of convective terms

Convective terms, such as the last integral on the RHS of (27), involve the computation of the spatial derivatives of stresses. Since the stress values are computed at the integration points, and not at the nodal points connecting the elements, the stress field is generally discontinuous across element edges. Thus, stress gradients cannot be reliably computed on the element level when evaluating element matrices. A method of finding a continuous stress field by interpolation was first used by Huétink [6]. In this method, integration point stresses are first extrapolated by a least square approximation to get the nodal stresses. Nodal stresses computed from each element are then averaged. A continuous stress field is then assumed in the form

$${}^t\sigma_{ij} = \sum_{\alpha=1}^{N} h_\alpha^t \sigma_{ij\alpha} \tag{30}$$

where h_α is the element shape function evaluated at node α, $\sigma_{ij\alpha}$ are the nodal stress components at node α and N is the number of element nodal points. Finally, the spatial derivatives of integration point stresses can be computed on the element level as

$$\frac{\partial {}^t\sigma_{ij}}{\partial {}^tx_k} = \sum_{\alpha=1}^{N} \frac{\partial h_\alpha}{\partial {}^tx_k}{}^t\sigma_{ij\alpha} \tag{31}$$

Another method for treating convective terms was proposed by Liu et al. [13]. A stress-velocity product is defined in the form

$${}^ty_{ijk} = ({}^tv_k - {}^tv_k^g){}^t\sigma_{ij} \tag{32}$$

Differentiating (32) with respect to space gives the convective term as

$$({}^tv_k - {}^tv_k^g)\frac{\partial {}^t\sigma_{ij}}{\partial {}^tx_k} = \frac{\partial {}^ty_{ijk}}{\partial {}^tx_k} - \left(\frac{\partial {}^tv_k}{\partial {}^tx_k} - \frac{\partial {}^tv_k^g}{\partial {}^tx_k}\right){}^t\sigma_{ij} \tag{33}$$

Equation (33) circumvents the computation of the stress gradients by computing the gradients of the stress-velocity product instead. However, this method necessitates the use of a weak form of stress integration to establish the nodal values for the stress-velocity product.

In this paper, a method for the treatment of the convective term that sidesteps the computation of the spatial gradients of stresses is used. This method involves a transformation from volume integrals to surface integrals as offered by the divergence theorem. Use is also made of the boundary constraint in (5). The last integral on the RHS of (27) can be rewritten as

$$\int_{{}^tV} (u_k - u_k^g)\frac{\partial {}^t\sigma_{ij}}{\partial {}^tx_k}\delta_t e_{ij}{}^t\mathrm{d}V = \int_{{}^tV} \frac{\partial[(u_k-u_k^g){}^t\sigma_{ij}\delta_t e_{ij}]}{\partial {}^tx_k}{}^t\mathrm{d}V - \int_{{}^tV} (u_k-u_k^g){}^t\sigma_{ij}\frac{\partial \delta_t e_{ij}{}^t}{\partial {}^tx_k}\mathrm{d}V - \int_{{}^tV}\left(\frac{\partial u_k}{\partial {}^tx_k}-\frac{\partial u_k^g}{\partial {}^tx_k}\right){}^t\sigma_{ij}\delta_t e_{ij}{}^t\mathrm{d}V \tag{34}$$

Applying the divergence theorem to the first integral in (34) and using (5), we get

$$\int_{{}^tV} \frac{\partial[(u_k-u_k^g){}^t\sigma_{ij}\delta_t e_{ij}]_t}{\partial {}^tx_k}\mathrm{d}V = \int_{{}^tS} (u_k-u_k^g){}^t\sigma_{ij}\delta_t e_{ij}{}^tn_k{}^t\mathrm{d}S = 0 \tag{35}$$

Substituting in (27), the internal virtual work becomes

$$\begin{aligned}\int_{t+\Delta t V} {}^{t+\Delta t}\sigma_{ij}\delta^{t+\Delta t}e_{ij}{}^{t+\Delta t}\mathrm{d}V &= \int_{{}^tV} {}^t\sigma_{ij}\delta_t e_{ij}{}^t\mathrm{d}V + \int_{{}^tV} {}^t\dot{\sigma}_{ij}\Delta t\delta_t e_{ij}{}^t\mathrm{d}V + \int_{{}^tV} {}^t\sigma_{ij}\delta_t e_{ij}\frac{\partial u_k}{\partial {}^tx_k}{}^t\,\mathrm{d}V \\ &\quad - \int_{{}^tV} \frac{\partial u_k^g}{\partial {}^tx_j}{}^t\sigma_{ij}\frac{\partial \delta u_i}{\partial {}^tx_k}{}^t\,\mathrm{d}V + \int_{{}^tV} (u_k-u_k^g){}^t\sigma_{ij}\frac{\partial \delta_t e_{ij}}{\partial {}^tx_k}{}^t\mathrm{d}V\end{aligned} \tag{36}$$

The same method can be applied to the convective body force term to avoid the computation of the spatial derivatives of density. The last integral on the RHS of (28) can be treated in the same manner as in (34) and (35), to give

$$\begin{aligned}\int_{t+\Delta t V} {}^{t+\Delta t}\rho^{t+\Delta t}f_i^{\mathrm{B}}\delta u_i{}^{t+\Delta t}\mathrm{d}V &= \int_{{}^tV} {}^t\rho^{t+\Delta t}f_i^{\mathrm{B}}\delta u_i{}^t\mathrm{d}V + \int_{{}^tV} {}^t\rho\frac{\partial^{t+\Delta t}f_i^{\mathrm{B}}}{\partial {}^tx_k}(u_k-u_k^g)\delta u_i{}^t\mathrm{d}V \\ &\quad + \int_{{}^tV} {}^t\rho^{t+\Delta t}f_i^{\mathrm{B}}(u_k-u_k^g)\frac{\partial \delta u_i{}^t}{\partial {}^tx_k}\mathrm{d}V\end{aligned} \tag{37}$$

3.5
Fully coupled ALE equilibrium equation

Substituting by (36), (37) and (29) into (12), the principle of virtual displacements at time $t+\Delta t$ referred to time t can be written as

$$\begin{aligned}
&\int_{{}^tV} {}^t\dot{\sigma}_{ij}\Delta t\delta_t e_{ij}{}^t\,\mathrm{d}V + \int_{{}^tV} {}^t\sigma_{ij}\delta_t e_{ij}\frac{\partial u_k}{\partial {}^t x_k}{}^t\mathrm{d}V \\
&+ \int_{{}^tV} (u_k - u_k^g){}^t\sigma_{ij}\frac{\partial \delta_t e_{ij}}{\partial {}^t x_k}{}^t\mathrm{d}V \\
&- \int_{{}^tV} \frac{\partial u_k^g}{\partial {}^t x_j}{}^t\sigma_{ij}\frac{\partial \delta u_i}{\partial {}^t x_k}{}^t\mathrm{d}V \\
&= \delta^{t+\Delta t}W^{\mathrm{ext}} - \int_{{}^tV} {}^t\sigma_{ij}\delta_t e_{ij}{}^t\mathrm{d}V
\end{aligned} \tag{38}$$

where

$$\begin{aligned}
\delta^{t+\Delta t}W^{\mathrm{ext}} &= \int_{{}^tV} {}^t\rho^{t+\Delta t}f_i^{\mathrm{B}}\delta u_i{}^t\mathrm{d}V \\
&+ \int_{{}^tV} {}^t\rho\frac{\partial^{t+\Delta t}f_i^{\mathrm{B}}}{\partial {}^t x_k}(u_k - u_k^g)\delta u_i{}^t\mathrm{d}V \\
&+ \int_{{}^tV} {}^t\rho^{t+\Delta t}f_i^{\mathrm{B}}(u_k - u_k^g)\frac{\partial \delta u_i}{\partial {}^t x_k}{}^t\mathrm{d}V \\
&+ \int_{{}^tS} {}^{t+\Delta t}f_i^S\left[1 + \frac{\partial u_k^g}{\partial {}^t x_k} - \frac{1}{2}\left(\frac{\partial u_m^g}{\partial {}^t x_n} + \frac{\partial u_n^g}{\partial {}^t x_m}\right){}^t n_m{}^t n_n\right]\delta u_i{}^t\mathrm{d}S
\end{aligned} \tag{39}$$

Equation (38) represents the fully coupled ALE equilibrium equation. This equation can reduce to the updated Lagrangian formulation if we choose to attach the grid to the material, i.e. $u_i^g = u_i$, and to the Eulerian formulation if we choose to fix the grid in space, i.e. $u_i^g = 0$, as limiting cases. The constitutive relations in (19) to (21) can now be introduced into the first integral in (38) to give

$$\begin{aligned}
&\int_{{}^tV} {}^tC_{ijklt}^{\mathrm{EP}}e_{kl}\delta_t e_{ij}{}^t\,\mathrm{d}V + \int_{{}^tV} {}^t\sigma_{ij}\delta_t\eta_{ij}{}^t\mathrm{d}V \\
&+ \int_{{}^tV} (u_k - u_k^g){}^t\sigma_{ij}\frac{\partial \delta_t e_{ij}}{\partial {}^t x_k}{}^t\mathrm{d}V \\
&+ \int_{{}^tV} \left(\frac{\partial u_k}{\partial {}^t x_j} - \frac{\partial u_k^g}{\partial {}^t x_j}\right){}^t\sigma_{ij}\frac{\partial \delta u_i}{\partial {}^t x_k}{}^t\mathrm{d}V \\
&= \delta^{t+\Delta t}W^{\mathrm{ext}} - \int_{{}^tV} {}^t\sigma_{ij}\delta_t e_{ij}{}^t\mathrm{d}V
\end{aligned} \tag{40}$$

where

$${}_t\eta_{ij} = \frac{1}{2}\frac{\partial u_k}{\partial {}^t x_i}\frac{\partial u_k}{\partial {}^t x_j} \tag{41}$$

The first two integrals on the LHS of (40) are exactly the same as those obtained using the updated Lagrangian formulation. The last two integrals on the LHS are the contributions to the stiffness matrix induced by mesh motion.

4
Dynamic analysis

4.1
Virtual work done by inertia forces

In dynamic analyses, inertia effects are included in the balance of momentum at time $t+\Delta t$. Inertia forces involve the material time derivative of material velocities, i.e. material accelerations ${}^{t+\Delta t}\dot{v}_i$. In the ALE formulation, we follow the grid point in its motion as our reference configuration. Therefore, the material referential acceleration, which is the grid time derivative of the material velocity ${}^{t+\Delta t}v_i'$, should be used. For clarity, we will denote the material referential acceleration ${}^{t+\Delta t}v_i'$ by ${}^{t+\Delta t}a_i$.

Using the relation between the two time derivatives in (8), the virtual work done by inertia forces can be expanded as

$$\begin{aligned}
&\int_{{}^{t+\Delta t}V} {}^{t+\Delta t}\rho^{t+\Delta t}\dot{v}_i\delta u_i{}^{t+\Delta t}\mathrm{d}V \\
&= \int_{{}^{t+\Delta t}V} {}^{t+\Delta t}\rho^{t+\Delta t}a_i\delta u_i{}^{t+\Delta t}\mathrm{d}V \\
&\quad + \int_{{}^{t+\Delta t}V} {}^{t+\Delta t}\rho({}^{t+\Delta t}v_j - {}^{t+\Delta t}v_j^g)\frac{\partial^{t+\Delta t}v_i}{\partial^{t+\Delta t}x_j}\delta u_i{}^{t+\Delta t}\mathrm{d}V
\end{aligned} \tag{42}$$

Equation (42) is considered as an extra virtual work term due to inertia effects to be added to the LHS, or subtracted from the RHS, of the ALE virtual work equation, (40). The first term on the RHS of (42) can be referred to as the referential inertia term whereas the second term is referred to as the convective inertia term.

4.2
Decomposition of velocities and accelerations

The velocities and accelerations at time $t+\Delta t$ can be related to their respective values at time t using the relations

$${}^{t+\Delta t}a_i = {}^ta_i + a_i \tag{43}$$

$${}^{t+\Delta t}v_i = {}^tv_i + v_i \tag{44}$$

$${}^{t+\Delta t}v_i^g = {}^tv_i^g + v_i^g \tag{45}$$

where the incremental quantities a_i, v_i and v_i^g depends on the implicit time integration scheme to be employed. Higher orders in a_i, v_i, v_i^g and Δt will be neglected during linearization.

4.3
Linearization of the referential inertia term

Incremental decomposition of the variables in the referential inertia term, in a manner similar to quasi-static analysis and linearization of the result gives

$$\begin{aligned}
&\int_{t+\Delta t V} {}^{t+\Delta t}\rho\, {}^{t+\Delta t}a_i \delta u_i\, {}^{t+\Delta t}\mathrm{d}V \\
&\quad = \int_{{}^{t}V} {}^{t}\rho\, {}^{t+\Delta t}a_i \delta u_i\, {}^{t}\mathrm{d}V \\
&\qquad - \int_{{}^{t}V} {}^{t}\rho \left(\frac{\partial^t v_k}{\partial^t x_k} - \frac{\partial^t v_k^g}{\partial^t x_k} \right)^{t+\Delta t} a_i \delta u_i \Delta t^t \mathrm{d}V \\
&\qquad - \int_{{}^{t}V} \frac{\partial^t \rho}{\partial^t x_k} \left({}^{t}v_k - {}^{t}v_k^g \right)^{t+\Delta t} a_i \delta u_i \Delta t\, {}^{t}\mathrm{d}V \qquad (46)
\end{aligned}$$

The last integral on the RHS of (46) can be rewritten as

$$\begin{aligned}
&\int_{{}^{t}V} \frac{\partial^t \rho}{\partial^t x} \left({}^{t}v_k - {}^{t}v_k^g \right)^{t+\Delta t} a_i \delta u_i \Delta t^t \mathrm{d}V \\
&\quad = \int_{{}^{t}V} \frac{\partial \left[{}^{t}\rho ({}^{t}v_k - {}^{t}v_k^g)^{t+\Delta t} a_i \delta u_i \right]}{\partial^t x_k} \Delta t^t \mathrm{d}V \\
&\qquad - \int_{{}^{t}V} {}^{t}\rho \left(\frac{\partial^t v_k}{\partial^t x_k} - \frac{\partial^t v_k^g}{\partial^t x_k} \right)^{t+\Delta t} a_i \delta u_i \Delta t^t \mathrm{d}V \\
&\qquad - \int_{{}^{t}V} {}^{t}\rho \left({}^{t}v_k - {}^{t}v_k^g \right) \frac{\partial ({}^{t+\Delta t}a_i \delta u_i)}{\partial^t x_k} \Delta t^t \mathrm{d}V \qquad (47)
\end{aligned}$$

Applying the divergence theorem to the first integral above and using the boundary constraint in (5), we get

$$\begin{aligned}
&\int_{{}^{t}V} \frac{\partial \left[{}^{t}\rho ({}^{t}v_k - {}^{t}v_k^g)^{t+\Delta t} a_i \delta u_i \right]}{\partial^t x_k} \Delta t^t \, \mathrm{d}V \\
&\quad = \int_{{}^{t}S} {}^{t}\rho ({}^{t}v_k - {}^{t}v_k^g)^{t+\Delta t} a_i \delta u_i n_k \Delta t^t \mathrm{d}V = 0 \qquad (48)
\end{aligned}$$

Substituting in (46), we get

$$\begin{aligned}
&\int_{t+\Delta t V} {}^{t+\Delta t}\rho\, {}^{t+\Delta t}a_i \delta u_i\, {}^{t+\Delta t}\mathrm{d}V \\
&\quad = \int_{{}^{t}V} {}^{t}\rho\, {}^{t+\Delta t}a_i \delta u_i\, {}^{t}\mathrm{d}V \\
&\qquad + \int_{{}^{t}V} {}^{t}\rho ({}^{t}v_k - {}^{t}v_k^g) \frac{(\partial^{t+\Delta t} a_i \delta u_i)}{\partial^t x_k} \Delta t^t \mathrm{d}V \qquad (49)
\end{aligned}$$

Using (43), the referential inertia term can be written as

$$\begin{aligned}
&\int_{t+\Delta t V} {}^{t+\Delta t}\rho\, {}^{t+\Delta t}a_i \delta u_i\, {}^{t+\Delta t}\mathrm{d}V \\
&\quad = \int_{{}^{t}V} {}^{t}\rho\, {}^{t}a_i \delta u_i\, {}^{t}\mathrm{d}V + \int_{{}^{t}v} {}^{t}\rho a_i \delta u_i\, {}^{t}\mathrm{d}V \\
&\qquad + \int_{{}^{t}V} {}^{t}\rho ({}^{t}v_k - {}^{t}v_k^g) \frac{\partial ({}^{t}a_i \delta u_i)}{\partial^t x_k} \Delta t^t \mathrm{d}V \qquad (50)
\end{aligned}$$

4.4
Linearization of the convective inertia term

In the incremental decomposition and linearization of the convective inertia term, it can be shown that

$$\frac{\partial^{t+\Delta t} v_i}{\partial^{t+\Delta t} x_j} = \frac{\partial^{t+\Delta t} v_i}{\partial^t x_j} - \frac{\partial^{t+\Delta t} v_i}{\partial^t x_k} \frac{\partial^t v_k}{\partial^t x_j} \Delta t \qquad (51)$$

The convective inertia term can be expanded as

$$\begin{aligned}
&\int_{t+\Delta t V} {}^{t+\Delta t}\rho ({}^{t+\Delta t}v_j - {}^{t+\Delta t}v_j^g) \frac{\partial^{t+\Delta t} v_i}{\partial^{t+\Delta t} x_j} \delta u_i\, {}^{t+\Delta t}\mathrm{d}V \\
&\quad = \int_{{}^{t}V} {}^{t}\rho ({}^{t+\Delta t}v_j - {}^{t+\Delta t}v_j^g) \frac{\partial^{t+\Delta t} v_i}{\partial^t x_j} \delta u_i\, {}^{t}\mathrm{d}V \\
&\qquad - \int_{{}^{t}V} {}^{t}\rho \left(\frac{\partial^t v_k}{\partial^t x_k} - \frac{\partial^t v_k^g}{\partial^t x_k} \right) ({}^{t+\Delta t}v_j - {}^{t+\Delta t}v_j^g) \frac{\partial^{t+\Delta t} v_i}{\partial^t x_j} \delta u_i \Delta t^t \mathrm{d}V \\
&\qquad - \int_{{}^{t}V} \frac{\partial^t \rho}{\partial^t x_k} ({}^{t}v_k - {}^{t}v_k^g) ({}^{t+\Delta t}v_j - {}^{t+\Delta t}v_j^g) \frac{\partial^{t+\Delta t} v_i}{\partial^t x_j} \delta u_i \Delta t^t \mathrm{d}V \\
&\qquad - \int_{{}^{t}V} {}^{t}\rho \frac{\partial^t v_k^g}{\partial^t x_j} ({}^{t+\Delta t}v_j - {}^{t+\Delta t}v_j^g) \frac{\partial^{t+\Delta t} v_i}{\partial^t x_k} \delta u_i \Delta t^t \mathrm{d}V \qquad (52)
\end{aligned}$$

As before the third integral above, which involves the spatial gradients of density, can be treated using the divergence theorem and the boundary constraint, to get

$$\begin{aligned}
&\int_{t+\Delta t V} {}^{t+\Delta t}\rho ({}^{t+\Delta t}v_j - {}^{t+\Delta t}v_j^g) \frac{\partial^{t+\Delta t} v_i}{\partial^{t+\Delta t} x_j} \delta u_i\, {}^{t+\Delta t}\mathrm{d}V \\
&\quad = \int_{{}^{t}V} {}^{t}\rho ({}^{t+\Delta t}v_j - {}^{t+\Delta t}v_j^g) \frac{\partial^{t+\Delta t} v_i}{\partial^t x_j} \delta u_i\, {}^{t}\mathrm{d}V \\
&\qquad + \int_{{}^{t}V} {}^{t}\rho ({}^{t}v_k - {}^{t}v_k^g) \left(\frac{\partial^{t+\Delta t} v_j}{\partial^t x_k} - \frac{\partial^{t+\Delta t} v_j^g}{\partial^t x_k} \right) \\
&\qquad \times \frac{\partial^{t+\Delta t} v_i}{\partial^t x_j} \delta u_i \Delta t^t \mathrm{d}V
\end{aligned}$$

$$+\int_{{}^tV}{}^t\rho({}^tv_k-{}^tv_k^g)({}^{t+\Delta t}v_j-{}^{t+\Delta t}v_j^g)\times\frac{\partial}{\partial^t x_k}\left(\frac{\partial^{t+\Delta t}v_i}{\partial^t x_j}\delta u_i\right)\Delta t^t\mathrm{d}V-\int_{{}^tV}{}^t\rho\frac{\partial^t v_k^g}{\partial^t x_j}({}^{t+\Delta t}v_j-{}^{t+\Delta t}v_j^g)\frac{\partial^{t+\Delta t}v_i}{\partial^t x_k}\delta u_i\Delta t^t\mathrm{d}V \tag{53}$$

Using (44) and (45), the convective inertia term can be written as

$$\begin{aligned}&\int_{{}^{t+\Delta t}V}{}^{t+\Delta t}\rho({}^{t+\Delta t}v_j-{}^{t+\Delta t}v_j^g)\frac{\partial^{t+\Delta t}v_i}{\partial^{t+\Delta t}x_j}\delta u_i{}^{t+\Delta t}\mathrm{d}V\\&=\int_{{}^tV}{}^t\rho({}^tv_j-{}^tv_j^g)\frac{\partial^t v_i}{\partial^t x_j}\delta u_i{}^t\mathrm{d}V+\int_{{}^tV}{}^t\rho({}^tv_j-{}^tv_j^g)\frac{\partial v_i}{\partial^t x_j}\delta u_i{}^t\mathrm{d}V+\int_{{}^tV}{}^t\rho(v_j-v_j^g)\frac{\partial^t v_i}{\partial^t x_j}\delta u_i{}^t\mathrm{d}V+\int_{{}^tV}{}^t\rho({}^tv_k-{}^tv_k^g)\\&\times\left(\frac{\partial^t v_j}{\partial^t x_k}-2\frac{\partial^t v_j^g}{\partial^t x_k}\right)\frac{\partial^t v_i}{\partial^t x_j}\delta u_i\Delta t^t\mathrm{d}V+\int_{{}^tV}{}^t\rho({}^tv_k-{}^tv_k^g)({}^tv_j-{}^tv_j^g)\frac{\partial}{\partial^t x_k}\left(\frac{\partial^t v_i}{\partial^t x_j}\delta u_i\right)\Delta t^t\mathrm{d}V\end{aligned} \tag{54}$$

4.5
Fully coupled ALE equation of motion

Combining (40), (50) and (54), the fully coupled ALE equation of motion can be written as

$$\begin{aligned}&\int_{{}^tV}{}^t\rho a_i\delta u_i{}^t\mathrm{d}V+\int_{{}^tV}{}^tC^{\mathrm{EP}}_{ijkl}{}^te_{kl}\delta_t e_{ij}{}^t\mathrm{d}V+\int_{{}^tV}{}^t\sigma_{ij}\delta_t\eta_{ij}{}^t\mathrm{d}V+\int_{{}^tV}{}^t\rho({}^tv_j-{}^tv_j^g)\frac{\partial v_i}{\partial^t x_j}\delta u_i{}^t\mathrm{d}V\\&+\int_{{}^tV}{}^t\rho(v_j-v_j^g)\frac{\partial^t v_i}{\partial^t x_j}\delta u_i{}^t\mathrm{d}V+\int_{{}^tV}(u_k-u_k^g)^t\sigma_{ij}\frac{\partial\delta_t e_{ij}}{\partial^t x_k}{}^t\mathrm{d}V+\int_{{}^tV}\left(\frac{\partial u_k}{\partial^t x_j}-\frac{\partial u_k^g}{\partial^t x_j}\right)^t\sigma_{ij}\frac{\partial\delta u_i}{\partial^t x_k}{}^t\mathrm{d}V\\&=\delta^{t+\Delta t}W^{\mathrm{ext}}-\int_{{}^tV}{}^t\sigma_{ij}\delta_t e_{ij}{}^t\,\mathrm{d}V-\int_{{}^tV}{}^t\rho^t a_i\delta u_i{}^t\mathrm{d}V-\int_{{}^tV}{}^t\rho({}^tv_k-{}^tv_k^g)\frac{\partial({}^ta_i\delta u_i)}{\partial^t x_k}\Delta t^t\mathrm{d}V\\&-\int_{{}^tV}{}^t\rho({}^tv_j-{}^tv_j^g)\frac{\partial^t v_i}{\partial^t x_j}\delta u_i{}^t\mathrm{d}V-\int_{{}^tV}{}^t\rho({}^tv_k-{}^tv_k^g)\times\left(\frac{\partial^t v_j}{\partial^t x_k}-2\frac{\partial^t v_j^g}{\partial^t x_k}\right)\frac{\partial^t v_i}{\partial^t x_j}\delta u_i\Delta t^t\mathrm{d}V\\&-\int_{{}^tV}{}^t\rho({}^tv_k-{}^tv_k^g)({}^tv_j-{}^tv_j^g)\times\frac{\partial}{\partial^t x_k}\left(\frac{\partial^t v_i}{\partial^t x_j}\delta u_i\right)\Delta t^t\mathrm{d}V\end{aligned} \tag{55}$$

The first three terms on both the LHS and RHS of (55) are exactly the same as in the updated Lagrangian formulation. The extra terms are due to ALE. Equation (55) shows that ALE can be considered as a logical extension to the updated Lagrangian formulation and the modifications to the equation of motion of current Lagrangian codes are clearly presented.

5
Mesh motion

5.1
Grid displacement

Using the ALE formulation, the finite element mesh can be moved arbitrarily to maintain a homogeneous mesh and properly represent boundary conditions throughout the deformation process. In this work, good control over the mesh motion in different parts of the mesh was obtained by associating the grid displacement with the material displacement by the following relation

$$u_i^g=\alpha_i+B_{ij}u_j \tag{56}$$

where α_i and B_{ij} are a vector and a matrix of mesh motion parameters, respectively. Vector α_i consists of appropriate grid displacements given by the mesh motion scheme while matrix B_{ij} consists of factors that allow the coupling of grid and material displacements. B_{ij} is usually chosen to

be a diagonal matrix, i.e. grid and material displacements are coupled only at the same degree of freedom. On free material boundaries however, it is sometimes necessary that all degrees of freedom of grid and material displacements be coupled at the same node. For two-dimensional problems, this would result in B_{ij} being a tridiagonal matrix. The motion of grid points in different parts of the mesh is controlled by the choice of the mesh motion parameters α_i and B_{ij} for each degree of freedom i as follows:

- For a pure Lagrangian degree of freedom: $\alpha_i = 0$ and $B_{ij} = \delta_{ij}$.
- For a pure Eulerian degree of freedom: $\alpha_i = 0$ and $B_{ij} = 0$.
- For an ALE degree of freedom: $\alpha_i$and B_{ij} are arbitrary.

5.2
Transfinite mapping

In this work, the transfinite mapping method [4] is used as the mesh motion scheme for the degrees of freedom interior to any mesh region with four known boundary curves. This method provides a homogeneous mesh and matches the boundary of a given region at an infinite number of points. Another distinct advantage of the transfinite mapping method is that it allows the discrete representation of boundary curves, i.e. the coordinates and displacements of boundary nodes can be used to find the optimum position of the nodes internal to the region. It also allows for discontinuities in slope of boundary curves.

The transfinite mapping algorithm starts by partitioning the initial mesh into a number of regions of simpler forms. Considering the mapping of a typical distorted mesh region bounded by four curves $\phi_i(r,0)$, $\phi_i(r,1)$, $\phi_i(0,s)$ and $\phi_i(1,s)$ as shown in Fig. 1, the new mesh coordinates can be obtained by mapping the region onto a unit square to give

$$\begin{aligned} {}^{t+\Delta t}x_i(r,s) = {} & (1-s)\phi_i(r,0) + s\phi_i(r,1) + (1-r)\phi_i(0,s) \\ & + r\phi_i(1,s) - (1-r)(1-s)\phi_i(0,0) \\ & - (1-r)s\phi_i(0,1) - rs\phi_i(1,1) \\ & - r(1-s)\phi_i(1,0) \end{aligned} \tag{57}$$

where $0 \le r \le 1$ and $0 \le s \le 1$ are the normalized coordinates over the region. Thus, the mesh motion parameter α_i for degree of freedom i internal to a region can be given by the transfinite mapping method as

$$\alpha_i = {}^{t+\Delta t}x_i - {}^{t}x_i \tag{58}$$

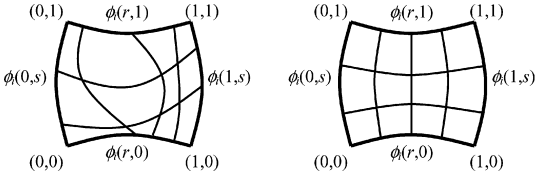

Fig. 1. Transfinite mapping of a distorted mesh region bounded by four curves

5.3
Mesh motion on free material boundaries

For the transfinite mapping method to give a good quality mesh within a certain region, grid points on the boundaries of this region must be uniformly distributed. Consider point k located on a 2-D free material boundary as shown in Fig. 2. Because of its location on a free material boundary, the ALE motion of point k is given by (56) as

$$u_x^g = \alpha_x + B_{xx}u_x + B_{xy}u_y \tag{59}$$

$$u_y^g = \alpha_y + B_{yx}u_x + B_{yy}u_y \tag{60}$$

where coupling between the x and y degrees of freedom is introduced in order that the grid motion of point k satisfies the boundary constraint given by equation (5). The question in this section is to find the mesh motion parameters α_x, B_{xx}, B_{xy}, α_y, B_{yx}, and B_{yy} for node k which satisfy the boundary constraint. We define a set of local axes $x'$and y'at grid point k such that x' is tangent to the boundary and y' is its normal. Assume that the local x' and y' axes at point k are inclined to the global x and y axes by an angle θ. The components of the incremental material and grid displacement vectors in the global and local coordinate systems are related by

$$u'_x = u_x \cos\theta + u_y \sin\theta \tag{61}$$

$$u'_y = -u_x \sin\theta + u_y \cos\theta \tag{62}$$

$$u'^g_x = u^g_x \cos\theta + u^g_y \sin\theta \tag{63}$$

$$u'^g_y = -u^g_x \sin\theta + u^g_y \cos\theta \tag{64}$$

Meanwhile, the mesh motion equations referred to the local coordinate system can be written as

$$u'^g_x = \alpha'_x + B'_{xx}u'_x + B'_{xy}u'_y \tag{65}$$

$$u'^g_y = \alpha'_y + B'_{yx}u'_x + B'_{yy}u'_y \tag{66}$$

where α'_x, B'_{xx} and B'_{xy} are the ALE mesh motion parameters in the direction tangent to the boundary and can be arbitrarily chosen while α'_y, B'_{yx} and B'_{yy} are in the direction normal to the boundary controlled by the boundary constraint. In this work, cubic spline interpolation is used to find new coordinates for point k such that all grid points on this free material boundary are

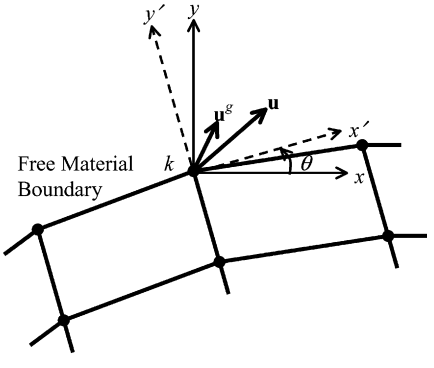

Fig. 2. Mesh motion on free material boundaries

uniformly distributed. The difference between the old and new coordinates for point k establishes the mesh motion parameter α'_x. In this case B'_{xx} and B'_{xy} can be set to zero. The boundary constraint dictates that $u'^g_y = u'_y$ thus giving $\alpha'_y = 0$, $B'_{yx} = 0$ and $B'_{yy} = 1$. Substituting (61), (62) and (63) into (65) and letting $B'_{xx} = B'_{xy} = 0$, we get

$$u^g_x \cos\theta + u^g_y \sin\theta = \alpha'_x \tag{67}$$

Substituting (61), (62) and (64) into (66), and applying the boundary constraint $\alpha'_y = 0$, $B'_{yx} = 0$ and $B'_{yy} = 1$, we get

$$-u^g_x \sin\theta + u^g_y \cos\theta = -u_x \sin\theta + u_y \cos\theta \tag{68}$$

Solving (67) and (68) for u^g_x and u^g_y, we get

$$u^g_x = \alpha'_x \cos\theta + u_x \sin^2\theta - u_y \sin\theta\cos\theta \tag{69}$$

$$u^g_y = \alpha'_x \sin\theta - u_x \sin\theta\cos\theta + u_y \cos^2\theta \tag{70}$$

Comparing equations (69) and (70) with equations (59) and (60), we get

$$\alpha_x = \alpha'_x \cos\theta \tag{71}$$

$$B_{xx} = \sin^2\theta \tag{72}$$

$$B_{xy} = -\sin\theta\cos\theta \tag{73}$$

$$\alpha_y = \alpha'_x \sin\theta \tag{74}$$

$$B_{yx} = -\sin\theta\cos\theta \tag{75}$$

$$B_{yy} = \cos^2\theta \tag{76}$$

The above ALE mesh motion parameters ensure that mesh motion on free material boundaries is consistent with the boundary constraint given by Eq. (5).

6 Finite element equations

6.1 Quasi-static analysis

Due to the approximations involved in the linearization of Eq. (40), an iteration procedure must be used to ensure equilibrium. Employing a modified Newton iteration, the matrix equation corresponding to (40) can be written for a single element or a group of elements as

$$({}^t\mathbf{K}^{L1} + {}^t\mathbf{K}^{L2})\mathbf{u}^{(i)} + ({}^t\mathbf{K}^{A1} + {}^t\mathbf{K}^{A2})(\mathbf{u}^{(i)} - \mathbf{u}^{g(i)}) = {}^{t+\Delta t}\mathbf{f}^{\text{ext}} - {}^{t+\Delta t}\mathbf{f}^{(i-1)} \tag{77}$$

where $\mathbf{u}^{(i)}$ and $\mathbf{u}^{g(i)}$ are the corrections to the incremental material and grid displacement vectors in iteration i and which are used to update displacements according to

$${}^{t+\Delta t}\mathbf{u}^{(i)} = {}^{t+\Delta t}\mathbf{u}^{(i-1)} + \mathbf{u}^{(i)} \tag{78}$$

$${}^{t+\Delta t}\mathbf{u}^{g(i)} = {}^{t+\Delta t}\mathbf{u}^{g(i-1)} + \mathbf{u}^{g(i)} \tag{79}$$

${}^t\mathbf{K}^{L1}$ and ${}^t\mathbf{K}^{L2}$ are the Lagrangian material and geometric stiffness matrices given by

$${}^t\mathbf{K}^{L1} = \int_{{}^tV} ({}_t\mathbf{B}^{L1})^{Tt}\,\mathbf{C}^{\text{EP}}\,{}_t\mathbf{B}^{L1t}\,\mathrm{d}V \tag{80}$$

$${}^t\mathbf{K}^{L2} = \int_{{}^tV} ({}_t\mathbf{B}^{L2})^{Tt}\,\mathbf{S}^{L2}\,{}_t\mathbf{B}^{L2t}\,\mathrm{d}V \tag{81}$$

in which ${}^t\mathbf{C}^{\text{EP}}$ is the elastic-plastic material constitutive matrix. ${}^t\mathbf{K}^{A1}$ and ${}^t\mathbf{K}^{A2}$ are the convective stiffness matrices due to ALE given by

$${}^t\mathbf{K}^{A1} = \int_{{}^tV} ({}_t\mathbf{B}^{A1})^{Tt}\,\mathbf{S}^{A1}\mathbf{H}^t\,\mathrm{d}V \tag{82}$$

$${}^t\mathbf{K}^{A2} = \int_{{}^tV} ({}_t\mathbf{B}^{A2})^{Tt}\,\mathbf{S}^{L2}\mathbf{B}^{L2t}\,\mathrm{d}V \tag{83}$$

${}^{t+\Delta t}\mathbf{f}^{(i-1)}$ is the internal force vector given by

$${}^{t+\Delta t}\mathbf{f}^{(i-1)} = \int_{{}^{t+\Delta t}V^{(i-1)}} \left({}_{t+\Delta t}\mathbf{B}^{L1(i-1)}\right)^{\mathrm{T}}\,{}^{t+\Delta t}\boldsymbol{\sigma}^{(i-1)}\,\mathrm{d}^{t+\Delta t}V \tag{84}$$

and ${}^{t+\Delta t}\mathbf{f}^{\text{ext}}$ is the vector of externally applied loads. The definition of matrices $\mathbf{H}$, ${}_t\mathbf{B}^{L1}$, ${}_t\mathbf{B}^{L2}$, ${}_t\mathbf{B}^{A1}$, ${}_t\mathbf{B}^{A2}$, ${}_t\mathbf{S}^{L2}$ and ${}_t\mathbf{S}^{A1}$ is given in Appendix A. It is clear from the third integral in Eq. (40) and from Appendix A, matrix ${}_t\mathbf{B}^{A1}$ involves second derivatives of shape functions. Thus, at least a C1-continuous representation of the shape functions is necessary for the accuracy of the results. Consequently only higher order elements were implemented in this work.

Equation (77) can be rewritten as

$$({}^t\mathbf{K}^L + {}^t\mathbf{K}^A)\mathbf{u}^{(i)} - {}^t\mathbf{K}^A\mathbf{u}^{g(i)} = {}^{t+\Delta t}\mathbf{f}^{\text{ext}} - {}^{t+\Delta t}\mathbf{f}^{(i-1)} \tag{85}$$

where

$${}^t\mathbf{K}^L = {}^t\mathbf{K}^{L1} + {}^t\mathbf{K}^{L2} \tag{86}$$

$${}^t\mathbf{K}^A = {}^t\mathbf{K}^{A1} + {}^t\mathbf{K}^{A2} \tag{87}$$

6.2 Dynamic analysis

Using the modified Newton iteration, the matrix equation corresponding to (55) can be written for a single element or a group of elements as

$$\begin{aligned} &{}^t\mathbf{M}^L\mathbf{a}^{(i)} + {}^t\mathbf{C}^{A1}\mathbf{v}^{(i)} + {}^t\mathbf{C}^{A2}(\mathbf{v}^{(i)} - \mathbf{v}^{g(i)}) \\ &\quad + ({}^t\mathbf{K}^{L1} + {}^t\mathbf{K}^{L2})\mathbf{u}^{(i)} + ({}^t\mathbf{K}^{A1} + {}^t\mathbf{K}^{A2}) \\ &\quad \times (\mathbf{u}^{(i)} - \mathbf{u}^{g(i)}) \\ &= {}^{t+\Delta t}\mathbf{f}^{\text{ext}} - {}^{t+\Delta t}\mathbf{f}^{(i-1)} \\ &\quad - ({}^t\mathbf{M}^L + {}^t\mathbf{M}^A)^{t+\Delta t}\mathbf{a}^{(i-1)} \\ &\quad - ({}^t\mathbf{C}^{A1} + {}^t\mathbf{C}^{A3} + {}^t\mathbf{C}^{A4})^{t+\Delta t}\mathbf{v}^{(i-1)} \end{aligned} \tag{88}$$

in which ${}^t\mathbf{M}^L$ is the Lagrangian mass matrix given by

$$ {}^t\mathbf{M}^L = \int_{{}^tV} {}^t\rho \mathbf{H}^{\mathrm{T}}\mathbf{H}\,{}^t\mathrm{d}V \tag{89} $$

and $\mathbf{a}^{(i)}$, $\mathbf{v}^{(i)}$ and $\mathbf{v}^{g(i)}$ are the corrections to the incremental material acceleration, material velocity and grid velocity vectors whereas ${}^{t+\Delta t}\mathbf{a}^{(i-1)}$ and ${}^{t+\Delta t}\mathbf{v}^{(i-1)}$ are the material acceleration and material velocity vectors at time $t+\Delta t$ iteration $i-1$. Next material acceleration, material velocity and grid velocity approximations are obtained using

$$ {}^{t+\Delta t}\mathbf{a}^{(i)} = {}^{t+\Delta t}\mathbf{a}^{(i-1)} + \mathbf{a}^{(i)} \tag{90} $$

$$ {}^{t+\Delta t}\mathbf{v}^{(i)} = {}^{t+\Delta t}\mathbf{v}^{(i-1)} + \mathbf{v}^{(i)} \tag{91} $$

$$ {}^{t+\Delta t}\mathbf{v}^{g(i)} = {}^{t+\Delta t}\mathbf{v}^{g(i-1)} + \mathbf{v}^{g(i)} \tag{92} $$

Appendix B gives the definition of the matrices ${}^t\mathbf{M}^A$, ${}^t\mathbf{C}^{A1}$, ${}^t\mathbf{C}^{A2}$, ${}^t\mathbf{C}^{A3}$ and ${}^t\mathbf{C}^{A4}$ related to the dynamic ALE equation. Equation (88) can be rewritten as

$$ \begin{aligned} &{}^t\mathbf{M}^L\mathbf{a}^{(i)} + ({}^t\mathbf{C}^{A1} + {}^t\mathbf{C}^{A2})\mathbf{v}^{(i)} \\ &\quad - {}^t\mathbf{C}^{A2}\mathbf{v}^{g(i)} + ({}^t\mathbf{K}^L + {}^t\mathbf{K}^A)\mathbf{u}^{(i)} - {}^t\mathbf{K}^A\mathbf{u}^{g(i)} \\ &= {}^{t+\Delta t}\mathbf{f}^{\mathrm{ext}} - {}^{t+\Delta t}\mathbf{f}^{(i-1)} \\ &\quad - ({}^t\mathbf{M}^L + {}^t\mathbf{M}^A)^{t+\Delta t}\mathbf{a}^{(i-1)} \\ &\quad - ({}^t\mathbf{C}^{A1} + {}^t\mathbf{C}^{A3} + {}^t\mathbf{C}^{A4})^{t+\Delta t}\mathbf{v}^{(i-1)} \end{aligned} \tag{93} $$

Equation (93) can be integrated using the Newmark implicit integration scheme in which the following two assumptions are used

$$ {}^{t+\Delta t}\mathbf{u}^{(i)} = {}^t\mathbf{u} + \Delta t\,{}^t\mathbf{v} + \Delta t^2\left(\frac{1}{2}-\beta\right){}^t\mathbf{a} + \Delta t^2\beta\,{}^{t+\Delta t}\mathbf{a}^{(i)} \tag{94} $$

$$ {}^{t+\Delta t}\mathbf{v}^{(i)} = {}^t\mathbf{v} + \Delta t(1-\gamma){}^t\mathbf{a} + \Delta t\gamma\,{}^{t+\Delta t}\mathbf{a}^{(i)} \tag{95} $$

where β and γ are parameters that control the integration accuracy and stability. Rearranging (94) we get,

$$ \begin{aligned} {}^{t+\Delta t}\mathbf{a}^{(i)} = \frac{1}{\Delta t^2\beta}\Big[&{}^{t+\Delta t}\mathbf{u}^{(i)} - {}^t\mathbf{u} \\ &-\Delta t\,{}^t\mathbf{v} - \Delta t^2\left(\frac{1}{2}-\beta\right){}^t\mathbf{a}\Big] \end{aligned} \tag{96} $$

Using (78)

$$ \begin{aligned} {}^{t+\Delta t}\mathbf{a}^{(i)} &= \frac{1}{\Delta t^2\beta}\Big[{}^{t+\Delta t}\mathbf{u}^{(i-1)} + \mathbf{u}^{(i)} - {}^t\mathbf{u} \\ &\quad -\Delta t\,{}^t\mathbf{v} - \Delta t^2\left(\frac{1}{2}-\beta\right){}^t\mathbf{a}\Big] \\ &= \frac{1}{\Delta t^2\beta}\Big[{}^{t+\Delta t}\mathbf{u}^{(i-1)} - {}^t\mathbf{u} \\ &\quad -\Delta t\,{}^t\mathbf{v} - \Delta t^2(\tfrac{1}{2}-\beta){}^t\mathbf{a}\Big] + \frac{1}{\Delta t^2\beta}\mathbf{u}^{(i)} \\ &= {}^{t+\Delta t}\mathbf{a}^{(i-1)} + \frac{1}{\Delta t^2\beta}\mathbf{u}^{(i)} \end{aligned} \tag{97} $$

Comparing (97) with (90) we get

$$ \mathbf{a}^{(i)} = \frac{1}{\Delta t^2\beta}\mathbf{u}^{(i)} \tag{98} $$

Substituting (97) into (95)

$$ \begin{aligned} {}^{t+\Delta t}\mathbf{v}^{(i)} &= {}^t\mathbf{v} + \Delta t(1-\gamma){}^t\mathbf{a} \\ &\quad + \Delta t\gamma\,{}^{t+\Delta t}\mathbf{a}^{(i-1)} + \Delta t\gamma\frac{1}{\Delta t^2\beta}\mathbf{u}^{(i)} \\ &= {}^{t+\Delta t}\mathbf{v}^{(i-1)} + \frac{\gamma}{\Delta t\beta}\mathbf{u}^{(i)} \end{aligned} \tag{99} $$

Comparing (99) with (91)

$$ \mathbf{v}^{(i)} = \frac{\gamma}{\Delta t\beta}\mathbf{u}^{(i)} \tag{100} $$

Similarly

$$ \mathbf{v}^{g(i)} = \frac{\gamma}{\Delta t\beta}\mathbf{u}^{g(i)} \tag{101} $$

Substituting (98) and (100) into (93) we get

$$ \begin{aligned} &\left[\frac{1}{\Delta t^2\beta}{}^t\mathbf{M}^L + \frac{\gamma}{\Delta t\beta}({}^t\mathbf{C}^{A1} + {}^t\mathbf{C}^{A2})\right. \\ &\quad \left.+({}^t\mathbf{K}^L + {}^t\mathbf{K}^A)\right]\mathbf{u}^{(i)} - \left[\frac{\gamma}{\Delta t\beta}{}^t\mathbf{C}^{A2} + {}^t\mathbf{K}^A\right]\mathbf{u}^{g(i)} \\ &= {}^{t+\Delta t}\mathbf{f}^{\mathrm{ext}} - {}^{t+\Delta t}\mathbf{f}^{(i-1)} \\ &\quad - ({}^t\mathbf{M}^L + {}^t\mathbf{M}^A)^{t+\Delta t}\mathbf{a}^{(i-1)} \\ &\quad - ({}^t\mathbf{C}^{A1} + {}^t\mathbf{C}^{A3} + {}^t\mathbf{C}^{A4})^{t+\Delta t}\mathbf{v}^{(i-1)} \end{aligned} \tag{102} $$

6.3 Condensation of grid displacement

Finite element equilibrium equations, Equation (85) for quasi-static analysis and Equation (102) for dynamic analysis, can both be written in the general form

$$ {}^t\mathbf{K}\mathbf{u}^{(i)} - {}^t\mathbf{K}^g\mathbf{u}^{g(i)} = \mathbf{f}^{(i)} \tag{103} $$

where ${}^t\mathbf{K}$ and ${}^t\mathbf{K}^g$ are equivalent stiffness matrices corresponding to $\mathbf{u}^{(i)}$ and $\mathbf{u}^{g(i)}$, respectively, while $\mathbf{f}^{(i)}$ is the incremental load vector for iteration i. Rewriting (56) in a matrix form

$$ \mathbf{u}^{g(i)} = \boldsymbol{\alpha} + \mathbf{B}\mathbf{u}^{(i)} \tag{104} $$

where $\boldsymbol{\alpha}$ and $\mathbf{B}$ are the vector and matrix of mesh motion parameters with the special cases of pure Lagrangian degrees of freedom given by $\boldsymbol{\alpha}=\mathbf{0}$ and $\mathbf{B}=\mathbf{I}$ and pure Eulerian degrees of freedom obtained by using $\boldsymbol{\alpha}=\mathbf{0}$ and $\mathbf{B}=\mathbf{0}$. The relation between the material and grid displacements in (104) is considered as a supplementary constraint equation to the finite element equilibrium equation (103). By introducing this constraint on the element level, grid displacements can be condensed out of element equilibrium equations prior to solution. Substituting (104) into (103), we get

$$ ({}^t\mathbf{K} - {}^t\mathbf{K}^g\mathbf{B})\mathbf{u}^{(i)} = \mathbf{f}^{(i)} + {}^t\mathbf{K}^g\boldsymbol{\alpha} \tag{105} $$

The conventional finite element assembly and elimination techniques may now be applied directly to solve for the material displacements. The only limitation to this procedure is that grid and material displacements may only be coupled at degrees of freedom within one element.

7
Construction of the elastic-plastic constitutive tensor

For rate-independent large strain elastic-plastic materials, the constitutive relation is generally given in terms of the rate of deformation tensor ${}^{t}D_{ij}$ and an objective stress rate such as the Truesdell stress rate ${}^{t}\sigma^{T}_{ij}$

$$ {}^{t}\sigma^{T}_{ij} = {}^{t}C^{\mathrm{EP}}_{ijkl}\,{}^{t}D_{kl} \tag{106} $$

where ${}^{t}C^{\mathrm{EP}}_{ijkl}$ is the instantaneous elastic-plastic constitutive tensor. The construction of the elastic-plastic tensor involves a yield condition, a flow rule and a hardening rule. In the classical theory of plasticity additive decomposition of the rate of formation tensor into elastic and plastic parts can be assumed in the form

$$ {}^{t}D_{ij} = {}^{t}D^{\mathrm{E}}_{ij} + {}^{t}D^{\mathrm{P}}_{ij} \tag{107} $$

in which the elastic part of the rate of deformation tensor ${}^{t}D^{\mathrm{E}}_{ij}$ can be related to the stress rate using

$$ \begin{aligned} {}^{t}\sigma^{T}_{ij} &= {}^{t}C^{\mathrm{E}}_{ijkl}\,{}^{t}D^{\mathrm{E}}_{kl} \\ &= {}^{t}C^{\mathrm{E}}_{ijkl}({}^{t}D_{kl} - {}^{t}D^{\mathrm{P}}_{kl}) \end{aligned} \tag{108} $$

where ${}^{t}C^{\mathrm{E}}_{ijkl}$ is the corresponding constitutive tensor of elastic moduli. Restricting the analysis to the associated flow rule, the plastic part of the rate of deformation tensor ${}^{t}D^{\mathrm{P}}_{ij}$ is given by

$$ {}^{t}D^{\mathrm{P}}_{ij} = {}^{t}\dot{\lambda}\frac{\partial {}^{t}f}{\partial {}^{t}\sigma_{ij}} \tag{109} $$

where ${}^{t}\dot{\lambda}$ is a scalar plastic flow rate and ${}^{t}f$ is the yield condition

$$ {}^{t}f({}^{t}\sigma_{ij}, {}^{t}q_k) = 0 \tag{110} $$

in which ${}^{t}q_k$ denotes a set of internal variables that characterize the hardening of the material such that

$$ {}^{t}\dot{q}_i = \dot{\lambda}\,{}^{t}h_i({}^{t}\sigma_{jk}, {}^{t}q_l) \tag{111} $$

During plastic loading, the stress is required to remain on the yield surface ${}^{t}\dot{f} = 0$. We also have ${}^{t}\dot{f} = 0$ which can be expanded using the chain rule to give

$$ \frac{\partial {}^{t}f}{\partial {}^{t}\sigma_{ij}}\,{}^{t}\dot{\sigma}_{ij} + \frac{\partial {}^{t}f}{\partial {}^{t}q_i}\,{}^{t}\dot{q}_i = 0 \tag{112} $$

The plastic consistency condition in (112) involves the material rate of Cauchy stresses ${}^{t}\dot{\sigma}_{ij}$ which upon transformation into the Truesdell rate and rearranging to solve for ${}^{t}\dot{\lambda}$ we get [15]

$$ {}^{t}\dot{\lambda} = \frac{\frac{\partial {}^{t}f}{\partial {}^{t}\sigma_{ij}}({}^{t}C^{\mathrm{E}}_{ijkl} + {}^{t}C^{*}_{ijkl})\,{}^{t}D_{kl}}{\frac{\partial {}^{t}f}{\partial {}^{t}\sigma_{qr}}\,{}^{t}C^{\mathrm{E}}_{qrst}\frac{\partial {}^{t}f}{\partial {}^{t}\sigma_{st}} - \frac{\partial {}^{t}f}{\partial {}^{t}q_u}\,{}^{t}h_u} \tag{113} $$

in which

$$ \begin{aligned} {}^{t}C^{*}_{ijkl} = \frac{1}{2}&(\delta_{ik}\,{}^{t}\sigma_{jl} + \delta_{il}\,{}^{t}\sigma_{jk} + \delta_{jk}\,{}^{t}\sigma_{il} + \delta_{jl}\,{}^{t}\sigma_{ik}) \\ &- \delta_{kl}\,{}^{t}\sigma_{ij} \end{aligned} \tag{114} $$

Substituting (113) into (109) and the result into (108) and comparing with (106) we get

$$ {}^{t}C^{\mathrm{EP}}_{ijkl} = {}^{t}C^{\mathrm{E}}_{ijkl} - \frac{{}^{t}C^{\mathrm{E}}_{ijop}\frac{\partial {}^{t}f}{\partial {}^{t}\sigma_{op}}\frac{\partial {}^{t}f}{\partial {}^{t}\sigma_{mn}}({}^{t}C^{\mathrm{E}}_{mnkl} + {}^{t}C^{*}_{mnkl})}{\frac{\partial {}^{t}f}{\partial {}^{t}\sigma_{qr}}\,{}^{t}C^{\mathrm{E}}_{qrst}\frac{\partial {}^{t}f}{\partial {}^{t}\sigma_{st}} - \frac{\partial {}^{t}f}{\partial {}^{t}q_u}\,{}^{t}h_u} \tag{115} $$

8
Stress update

For large deformation analysis, the algorithm for integrating the constitutive equations in time, also known as the stress update algorithm, should observe the material frame indifference, i.e., preserve the objectivity of the constitutive equations. For elastic-plastic materials, the algorithm should also satisfy the plastic consistency condition, i.e. keep the stress point at the end of the integration time step on the yield surface. The method used here is the common return mapping algorithm. The method consists of an elastic predictor step, in which a trial stress at time $t + \Delta t$ is computed by assuming pure elastic deformation, followed by a plastic corrector step in which the trial stress is projected onto an updated yield surface to satisfy the plastic consistency condition. Stress update can be readily treated in the case of the Lagrangian formulation because the element integration points are material points. In the ALE formulation, however, integration points do not coincide with material points and the stress needs to be convected by the relative velocity as indicated by Eq. (18).

One method of stress update is through the definition of the stress-velocity product given in Eq. (32) and integrating the weak form of the objective constitutive equations [13]. A discrete form of the constitutive equations is then obtained by defining a new set of shape functions to interpolate the stress and the stress-velocity product tensors. The stress objectivity consideration may be achieved using tensor transformation of the Cauchy stress tensor or by integration of the Truesdell stress rate.

In this work, the stress at time $t + \Delta t$ is assumed to be updated using

$$ \begin{aligned} {}^{t+\Delta t}\sigma_{ij} &= {}^{t}\sigma_{ij} + \Delta\sigma_{ij} \\ &= {}^{t}\sigma_{ij} + {}^{t+\Delta t}\sigma'_{ij}\Delta t \\ &= {}^{t}\sigma_{ij} + {}^{t+\Delta t}\dot{\sigma}_{ij}\Delta t - (u_k - u^{g}_k)\frac{\partial {}^{t}\sigma_{ij}}{\partial {}^{t+\Delta t}x_k} \\ &= {}^{t}\sigma_{ij} + \frac{\partial u_j}{\partial {}^{t+\Delta t}x_k}\,{}^{t}\sigma_{ik} + \frac{\partial u_i}{\partial {}^{t+\Delta t}x_k}\,{}^{t}\sigma_{jk} \\ &\quad - \frac{\partial u_k}{\partial {}^{t+\Delta t}x_k}\,{}^{t}\sigma_{ij} + {}^{t+\Delta t}\sigma^{T}_{ij}\Delta t \\ &\quad - (u_k - u^{g}_k)\frac{\partial {}^{t}\sigma_{ij}}{\partial {}^{t+\Delta t}x_k} \end{aligned} \tag{116} $$

where use have been made of the relations between the grid time derivative and the material rate of Cauchy stresses as well as the Truesdell stress rate given in Eqs. (18) and (19). The above relation can be rewritten in the form

$$^{t+\Delta t}\sigma_{ij} = {}^{t}\sigma_{ij} + \Delta\sigma_{ij}^{\text{rota}} + \Delta\sigma_{ij}^{\text{conv}} + {}^{t+\Delta t}\sigma_{ij}^{\text{T}}\Delta t \tag{117}$$

in which $\Delta\sigma_{ij}^{\text{rota}}$ represents a rotational objectivity term given by

$$\Delta\sigma_{ij}^{\text{rota}} = \frac{\partial u_j}{\partial^{t+\Delta t}x_k}{}^{t}\sigma_{ik} + \frac{\partial u_i}{\partial^{t+\Delta t}x_k}{}^{t}\sigma_{jk} - \frac{\partial u_k}{\partial^{t+\Delta t}x_k}{}^{t}\sigma_{ij} \tag{118}$$

whereas $\Delta\sigma_{ij}^{\text{conv}}$ is the ALE convective term given by

$$\Delta\sigma_{ij}^{\text{conv}} = -(u_k - u_k^g)\frac{\partial^t\sigma_{ij}}{\partial^{t+\Delta t}x_k} \tag{119}$$

and $^{t+\Delta t}\sigma_{ij}^{t}\Delta t$ is the incremental constitutive term given by

$$^{t+\Delta t}\sigma_{ij}^{T}\Delta t = {}^{t+\Delta t}C_{ijkl}^{\text{EP}}\,{}^{t+\Delta t}D_{kl}\Delta t \tag{120}$$

In the elastic predictor phase of the return mapping algorithm, the material behavior is assumed to be purely elastic and the incremental constitutive term is given by

$$^{t+\Delta t}\sigma_{ij}^{T}\Delta t = {}^{t+\Delta t}C_{ijkl}^{\text{E}}\,{}^{t+\Delta t}D^{\text{E}}{}_{kl}\Delta t \tag{121}$$

which upon using (107) gives

$$^{t+\Delta t}\sigma_{ij}^{T}\Delta t = {}^{t+\Delta t}C_{ijkl}^{\text{E}}({}^{t+\Delta t}D_{kl} - {}^{t+\Delta t}D_{kl}^{\text{P}})\Delta t \tag{122}$$

Substituting (122) into (117), the stress at time $t + \Delta t$ can be regrouped as

$$^{t+\Delta t}\sigma_{ij} = {}^{t+\Delta t}\sigma_{ij}^{\text{pred}} + \Delta\sigma_{ij}^{\text{corr}} + \Delta\sigma_{ij}^{\text{conv}} \tag{123}$$

in which $^{t+\Delta t}\sigma_{ij}^{\text{pred}}$ is the elastic predictor trial stress given by

$$^{t+\Delta t}\sigma_{ij}^{\text{pred}} = {}^{t}\sigma_{ij} + \Delta\sigma_{ij}^{\text{rota}} + {}^{t+\Delta t}C_{ijkl}^{\text{E}}\,{}^{t+\Delta t}D_{kl}\Delta t \tag{124}$$

and $\Delta\sigma_{ij}^{\text{corr}}$ is the plastic corrector stress increment given by

$$\Delta\sigma_{ij}^{\text{corr}} = -{}^{t+\Delta t}C_{ijkl}^{\text{E}}\,{}^{t+\Delta t}D_{kl}^{\text{P}}\Delta t \tag{125}$$

The plastic corrector phase projects the trial stress onto a suitably updated yield surface at time $t + \Delta t$ according to the flow and hardening rules. The evolution of the plastic corrector phase parameters is typically expressed in terms of a set of nonlinear algebraic equations that is linearized and solved using an iterative Newton procedure. It is worth noting that the variables are updated from the converged values at the end of the previous time step at time t and not from the nonconverged iterative values.

The convective term $\Delta\sigma_{ij}^{\text{conv}}$ given by (119) involves the computation of the spatial derivatives of stresses. To this end, the assumption of a continuous stress field as given by Eq. (30) is used in the computation. In defining $^{t+\Delta t}\sigma_{ij}^{\text{pred}}$ and $\Delta\sigma_{ij}^{\text{corr}}$ in Equation (123) for the ALE formulation, a decision had to be made on whether to include the convective term in the predictor phase only, the corrector phase only or in both phases. In this work, the convective stress term is chosen to be included at the end of the both phases to avoid possible numerical instabilities due to the arbitrariness of the grid motion. Numerical investigation into the relative accuracy of the other two approaches may be the topic of a future work.

9 Applications

9.1 One dimensional elastic-plastic stress wave problem

A finite element program based on the above ALE formulation has been developed. Several large strain metal forming examples have been solved using the program. In the first example, a wave propagation problem in a one-dimensional infinitely long elastic-plastic rod is used to test the ALE formulation with dynamic effects. The same problem was reported in [13] and [8]. It should be noted that this problem doesn't require an ALE analysis and was selected because of the availability of analytical and numerical solutions. The infinitely long rod is discretized using 400 elements with a mesh size of 0.1 units as shown in Fig. 3. The material properties of the rod are assumed to be: density = 10000.0, Young's modulus = 10000.0, plastic modulus = 3333.33, yield stress = 75.0 and Poisson's ratio = 0.0. The rod is subjected to a compressive stress wave 100.0 in amplitude and 4.5 in width. The stress wave and the time interval under consideration are depicted in Fig. 4.

Figures 5 and 6 compare the longitudinal stress distribution obtained using ALE with the analytical solution for both the elastic and elastic-plastic cases. ALE results are in good agreement with the analytical solution and with those of [13] and [8].

9.2 Sheet metal extrusion

Extrusion is a typical metal forming problem in which large strains are expected and in which remeshing and boundary condition updating are required if the traditional Lagrangian formulation is employed. In this problem, quasi-static plane strain sheet metal extrusion is simulated. The extrusion die produces a 25% reduction in

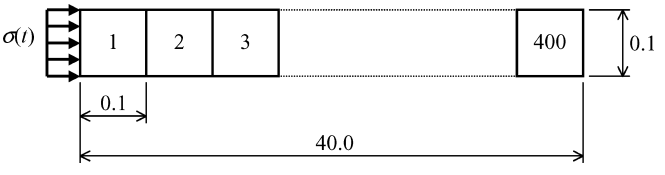

Fig. 3. Mesh for the one-dimensional wave propagation problem

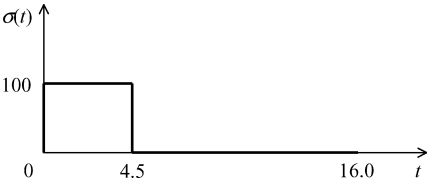

Fig. 4. Stress wave amplitude and duration for wave propagation problem

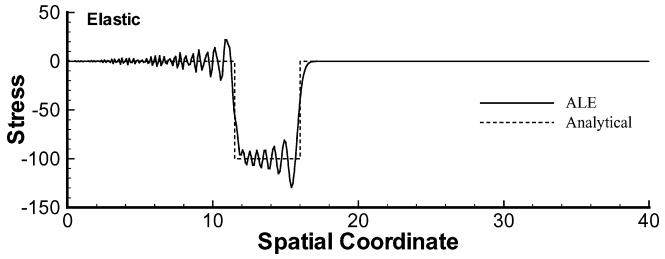

Fig. 5. Longitudinal stress distribution comparison, elastic case

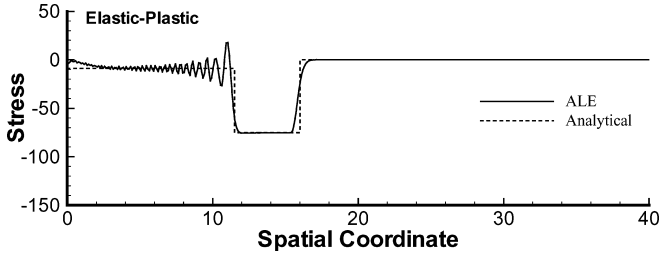

Fig. 6. Longitudinal stress distribution comparison, elastic–plastic case

sheet thickness and is shaped in the form of a 5th order polynomial with zero curvature and slope at both ends. An aluminum billet of thickness $2a$ is forced through the die by a rigid piston pressing against the rear face of the billet and moving with a prescribed displacement. The length of the die is taken as $1.2a$. The same problem was solved using the updated Lagrangian approach in [12]. The material properties for the aluminum billet are taken as: Young's modulus = 10^4 ksi, Poisson's ratio = 0.3, initial yield stress = 57 ksi and hardening parameter = 165 ksi. Figure 7 shows the initial geometry and mesh used in the simulation. Only the upper half of the billet was analyzed.

Using the ALE formulation, all the nodes confined to the die area are chosen to be Eulerian during the whole course of deformation. The nodes on the boundaries are taken as Lagrangian. The motion of all the other nodes is controlled by the ALE mesh motion scheme. Figure 8 shows the plastic strain distribution and the deformed shape after a piston displacement of $2a$ units. Contact between the billet and the die was set as boundary constraint equations. The ALE approach was able to eliminate the need for remeshing or boundary condition updating and the desired deformation level was reached without any user intervention or special contact treatments. Variations in the longitudinal stress component in the die region at

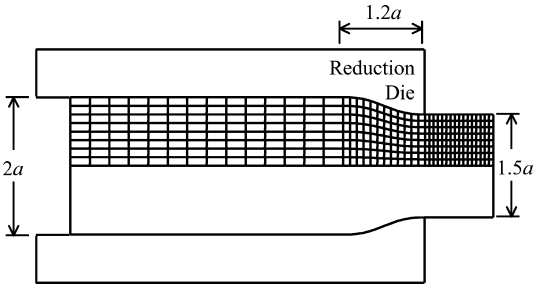

Fig. 7. Geometry and mesh for extrusion problem

different lateral positions from the mid-plane of the initial configuration are shown in Fig. 9. Results are in good agreement with those in [12].

9.3
Bar impact benchmark test

The bar impact problem has been investigated by many researchers [3, 10, 14, 18] and is considered a standard benchmark test for transient dynamic computer codes. In this problem, a cylindrical copper bar of initial radius 3.2 mm and length 32.4 mm strikes a rigid frictionless surface. The impact velocity is 227 m/s. The material is assumed to be elasto-plastic with Young's modulus = 117 GPa, plastic modulus = 100 MPa, Poisson's ratio = 0.35, initial yield stress = 400 MPa, and density = 8930 kg/m^3. A von Mises yield surface with linear isotropic hardening is assumed. Contact conditions are imposed by simply constraining the nodes in contact with the rigid surface. An axisymmetric mesh of 250 8-noded elements is used. Computations are carried out up to a time of 80 μs.

Figure 10 compares the deformed shape and finite element mesh obtained using both the Lagrangian and ALE formulations at different stages during the deformation process. In the ALE solution, boundary nodes are allowed to move in the tangential directions to the boundaries to maintain their uniform distribution while satisfying the ALE boundary constraint. The Lagrangian solution is obtained as a special case from the more general developed ALE formulation. It is clear that while the Lagrangian solution suffered severe mesh distortion, ALE was able to maintain a uniform mesh throughout the deformation history. Table 1 compares the final bar length and mushroom radius obtained using the developed code with numerical results obtained by other researchers. It is clear that the results obtained using the fully-coupled implicit dynamic ALE formulation are in agreement with other well-established numerical techniques and codes.

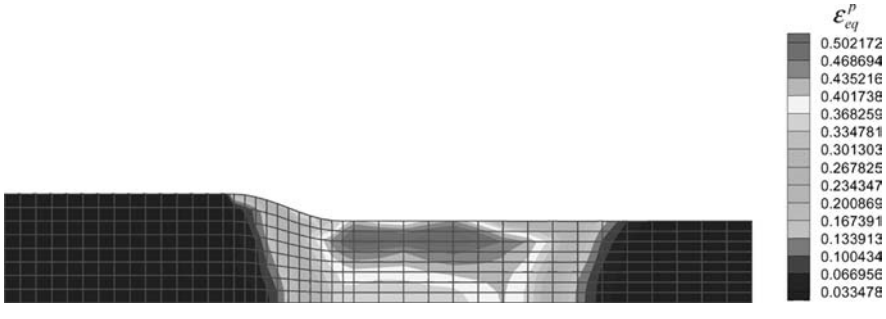

Fig. 8. Plastic strain contours and deformed shape for extrusion problem

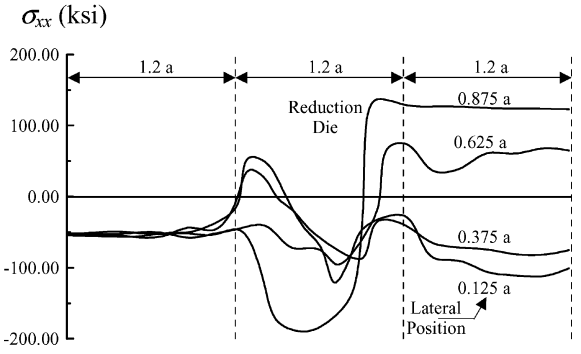

Fig. 9. Longitudinal stress at different lateral positions for extrusion problem

Figure 11 gives the equivalent stress and plastic strain contours.

9.4
Quasi-static and dynamic punch indentation

In this example, a punch indentation process is simulated to show the effectiveness of the ALE formulation in handling contact boundary conditions and in preventing mesh distortion. This process is simulated using both quasi-static and dynamic analyses to investigate the significance of dynamic effects. Figure 12 shows the geometry and initial mesh of the body. The workpiece is placed between two rigid frictionless tools moving with constant velocity under plane strain conditions. Because of symmetry, only one quarter of the domain is modeled. The deformation process is continued up to a 60% reduction of the original workpiece height. The material is assumed to be an elastic-plastic material with a Young's modulus of 200 GPa, a Poisson's ratio of 0.3, an initial yield stress of 250 MPa and a hardening parameter of 1 GPa.

Figure 13 shows the evolution of the deformed shape obtained using the developed ALE formulation. The figure shows that the contact condition between the punch and the workpiece is accurately satisfied. This was easily achieved by allowing the degrees of freedom of the nodes directly under the punch to be Lagrangian in the vertical direction (to satisfy the boundary constraint) and Eulerian in the horizontal direction (to maintain the same punch size under deformation). No special contact algorithm was needed to handle the contact conditions. In addition, ALE was able to maintain a homogeneous mesh throughout the deformation history.

The significance of dynamic effects is investigated by examining the indentation problem at different punch velocities. Figure 14 compares the final deformed shape and equivalent plastic strain distributions for the quasi-static case and for four different punch velocities. Dynamic effects are not significant for punch velocities less than 1 m/s since the deformed shape and plastic strain distribution are quite similar to those of the quasi-static simulation. One can also notice that low punch velocities allow the workpiece to flow horizontally away from the punch, while at high velocities the workpiece tends to back extrude.

10
Conclusions

In this paper, an implicit fully coupled ALE formulation for large deformation solid mechanics applications is presented. Starting from the basic principles of continuum mechanics, ALE equilibrium equations are derived for both quasi-static and dynamic analyses. A new method for the treatment of convective terms that sidesteps the computation of the spatial gradients of stresses is used in the derivation. Details of the finite element discretization are presented and full expressions for the resulting matrices and vectors for both quasi-static and dynamic analyses are given. Details of the mesh motion scheme and stress update are also presented. The developed formulation is implemented into a 2-D finite element code for elastic-plastic materials. Several quasi-static and dynamic large deformation problems are simulated using the program. The results show the effectiveness of the ALE approach in handling contact boundary conditions and in preventing mesh distortion.

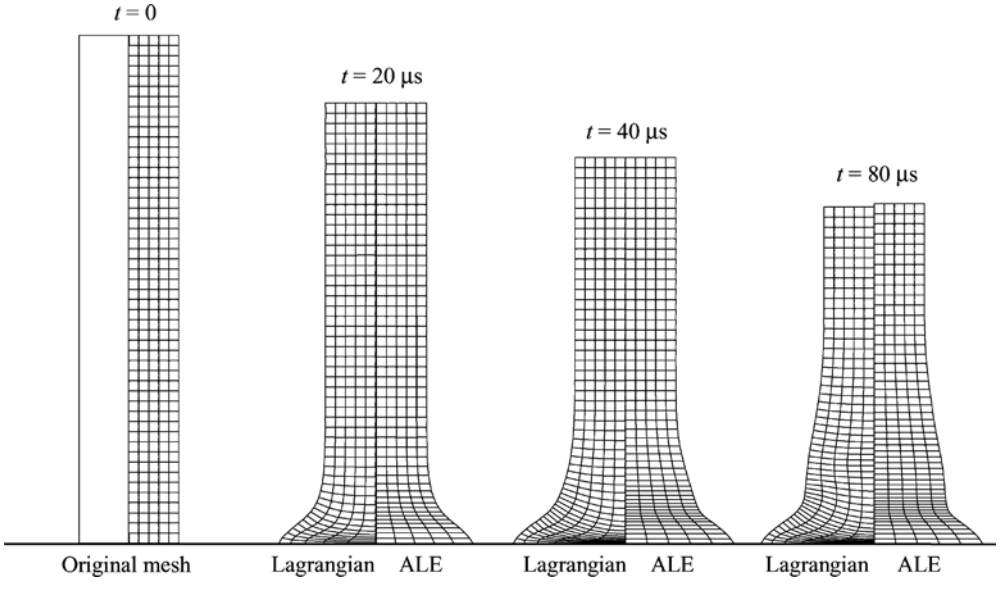

Fig. 10. Comparison of the Lagrangian and ALE solutions for bar impact problem

Table 1. Comparison of results for bar impact

Reference (Code/Method)	Final length (mm)	Final mushroom radius (mm)
Kamoulakos [10]		
MARC	21.66	7.02
DYNA2D	21.47	7.13
DYNA3D	21.47	7.03
NIKE2D	21.47	7.07
Zhu and Cescotto [18]		
Lagrangian (different element types)	21.26–21.49	6.97–7.18
Camacho and Ortiz [3]		
Lagrangian (different remeshing schemes)	21.42–21.44	7.21–7.24
Liu et al. [14]		
Lagrangian	21.42	7.15
ALE (explicit)	21.53	6.87
Current Work		
Lagrangian	21.48	7.22
ALE (implicit)	21.69	6.90

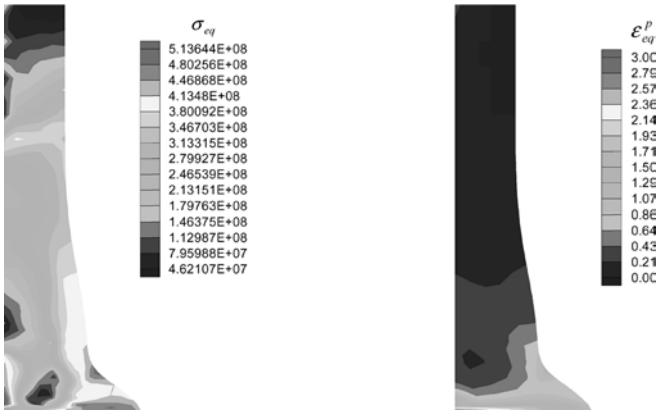

Fig. 11. Equivalent stress and plastic strain contours for bar impact problem

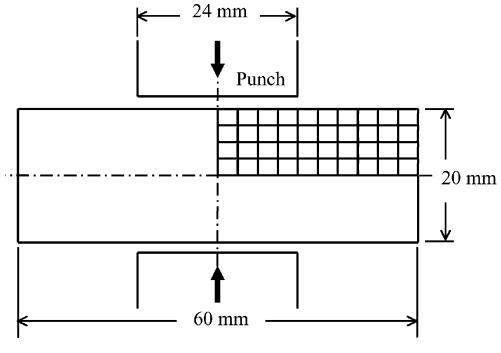

Fig. 12. Geometry and initial mesh for punch indentation problem

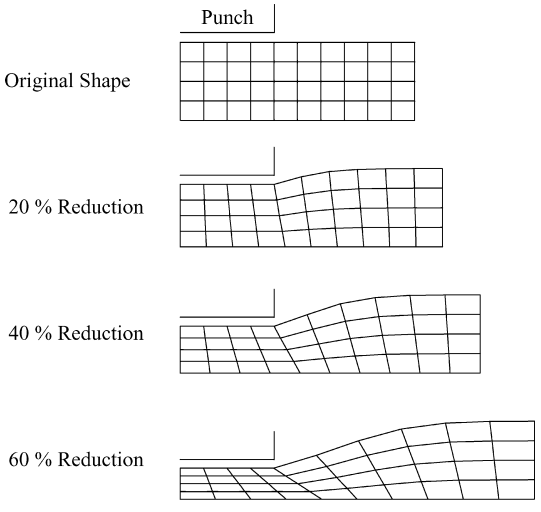

Fig. 13. Evolution of the deformed shape during the punch indentation problem

Appendix A
Matrices for 2-D quasi-static analysis

Letting h_k be the element shape function corresponding to nodal point k and N is the number of element nodal points, matrices $\mathbf{H}$, ${}_t\mathbf{B}^{L1}$, ${}_t\mathbf{B}^{L2}$, ${}_t\mathbf{B}^{A1}$, ${}_t\mathbf{B}^{A2}$, ${}_t\mathbf{S}^{L2}$ and ${}_t\mathbf{S}^{A1}$ are given by

$$\mathbf{H} = \begin{bmatrix} \cdots & h_k & 0 & \cdots \\ & 0 & h_k & \end{bmatrix}_{2\times 2N} \tag{A.1}$$

$${}_t\mathbf{B}^{L1} = \begin{bmatrix} & \frac{\partial h_k}{\partial {}^t x} & 0 & \\ & 0 & \frac{\partial h_k}{\partial {}^t y} & \\ \cdots & \frac{\partial h_k}{\partial {}^t y} & \frac{\partial h_k}{\partial {}^t x} & \cdots \\ & \frac{h_k}{\sum_{j=1}^{N} h_j {}^t\bar{x}_j} & 0 & \end{bmatrix}_{4\times 2N} \tag{A.2}$$

$${}_t\mathbf{B}^{L2} = \begin{bmatrix} & \frac{\partial h_k}{\partial {}^t x} & 0 & \\ & \frac{\partial h_k}{\partial {}^t y} & 0 & \\ & 0 & \frac{\partial h_k}{\partial {}^t x} & \\ \cdots & 0 & \frac{\partial h_k}{\partial {}^t y} & \cdots \\ & \frac{h_k}{\sum_{j=1}^{N} h_j {}^t\bar{x}_j} & 0 & \end{bmatrix}_{5\times 2N} \tag{A.3}$$

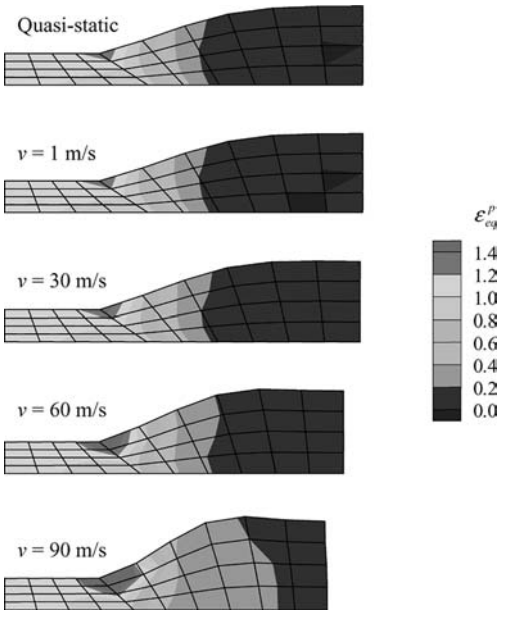

Fig. 14. Deformed shape and equivalent plastic strain at different punch velocities

$$ {}_t\mathbf{B}^{A1} = \begin{bmatrix} \frac{\partial^2 h_k}{\partial {}^t x^2} & 0 \\ \frac{\partial^2 h_k}{\partial {}^t y^2} & 0 \\ \frac{\partial^2 h_k}{\partial {}^t x \partial {}^t y} & 0 \\ 0 & \frac{\partial^2 h_k}{\partial {}^t x^2} \\ \cdots & \cdots \\ 0 & \frac{\partial^2 h_k}{\partial {}^t y^2} \\ 0 & \frac{\partial^2 h_k}{\partial {}^t x \partial {}^t y} \\ 0 & \left(\frac{1}{{}^t x}\frac{\partial h_k}{\partial {}^t x} - \frac{h_k}{{}^t x^2}\right) \\ 0 & \frac{1}{{}^t x}\frac{\partial h_k}{\partial {}^t y} \end{bmatrix}_{8\times 2N} \tag{A.4} $$

$$ {}_t\mathbf{B}^{A2} = \begin{bmatrix} \frac{\partial h_k}{\partial {}^t x} & 0 \\ 0 & \frac{\partial h_k}{\partial {}^t x} \\ \frac{\partial h_k}{\partial {}^t y} & 0 \\ \cdots & \cdots \\ 0 & \frac{\partial h_k}{\partial {}^t y} \\ \frac{h_k}{\sum_{j=1}^{N} h_j {}^t\bar{x}_j} & 0 \end{bmatrix}_{5\times 2N} \tag{A.5} $$

$$ {}^t\mathbf{S}^{L2} = \begin{bmatrix} {}^t\sigma_{xx} & {}^t\sigma_{xy} & 0 & 0 & 0 \\ {}^t\sigma_{xy} & {}^t\sigma_{yy} & 0 & 0 & 0 \\ 0 & 0 & {}^t\sigma_{xx} & {}^t\sigma_{xy} & 0 \\ 0 & 0 & {}^t\sigma_{xy} & {}^t\sigma_{yy} & 0 \\ 0 & 0 & 0 & 0 & {}^t\sigma_{zz} \end{bmatrix}_{5\times 5} \tag{A.6} $$

$$ {}^t\mathbf{S}^{A1} = \begin{bmatrix} {}^t\sigma_{xx} & 0 & {}^t\sigma_{xy} & {}^t\sigma_{xy} & 0 & {}^t\sigma_{yy} & {}^t\sigma_{zz} & 0 \\ 0 & {}^t\sigma_{xy} & {}^t\sigma_{xx} & 0 & {}^t\sigma_{yy} & {}^t\sigma_{xy} & 0 & {}^t\sigma_{zz} \end{bmatrix}^T_{2\times 8} \tag{A.7} $$

${}^{t+\Delta t}\boldsymbol{\sigma}^{(i-1)}$ is the stress vector defined by

$$ {}^{t+\Delta t}\boldsymbol{\sigma}^{(i-1)} = \begin{Bmatrix} {}^{t+\Delta t}\sigma_{xx}^{(i-1)} \\ {}^{t+\Delta t}\sigma_{yy}^{(i-1)} \\ {}^{t+\Delta t}\sigma_{xy}^{(i-1)} \\ {}^{t+\Delta t}\sigma_{zz}^{(i-1)} \end{Bmatrix} \tag{A.8} $$

Appendix B
Matrices for 2-D dynamic analysis

Matrix ${}^t\mathbf{M}^A$ is given by

$$ {}^t\mathbf{M}^A = \begin{bmatrix} & \vdots & \\ \cdots & {}^t M^A_{2i-1,2j-1} \quad {}^t M^A_{2i-1,2j} & \cdots \\ & {}^t M^A_{2i,2j-1} \quad {}^t M^A_{2i,2j} & \\ & \vdots & \end{bmatrix}_{2N\times 2N} \tag{B.1} $$

in which i and j indicate node numbers from 1 to N, and

$$ {}^t M^A_{2i-1,2j-1} = {}^t M^A_{2i,2j} = \int_{{}^tV} {}^t\rho \left[\left(h_i \frac{\partial h_j}{\partial {}^t x} + h_j \frac{\partial h_i}{\partial {}^t x} \right) \times \sum_{k=1}^{N} h_k \left({}^t\bar{v}_{xk} - {}^t\bar{v}^g_{xk} \right) + \left(h_i \frac{\partial h_j}{\partial {}^t y} + h_j \frac{\partial h_i}{\partial {}^t y} \right) \sum_{k=1}^{N} h_k \cdot \times \left({}^t\bar{v}_{yk} - {}^t\bar{v}^g_{yk} \right) \right] \Delta t \, {}^t\mathrm{d}V \tag{B.2} $$

$$ {}^t M^A_{2i-1,2j} = {}^t M^A_{2i,2j-1} = 0 \tag{B.3} $$

Matrix ${}^t\mathbf{C}^{A1}$ is given by

$$ {}^t\mathbf{C}^{A1} = \begin{bmatrix} & \vdots & \\ \cdots & {}^t C^{A1}_{2i-1,2j-1} \quad {}^t C^{A1}_{2i-1,2j} & \cdots \\ & {}^t C^{A1}_{2i,2j-1} \quad {}^t C^{A1}_{2i,2j} & \\ & \vdots & \end{bmatrix}_{2N\times 2N} \tag{B.4} $$

in which

$$ {}^t C^{A1}_{2i-1,2j-1} = {}^t C^{A1}_{2i,2j} = \int_{{}^tV} {}^t\rho h_i \left[\frac{\partial h_j}{\partial {}^t x} \sum_{k=1}^{N} h_k ({}^t\bar{v}_{xk} - {}^t\bar{v}^g_{xk}) + \frac{\partial h_j}{\partial {}^t y} \sum_{k=1}^{N} h_k ({}^t\bar{v}_{yk} - {}^t\bar{v}^g_{yk}) \right] {}^t\mathrm{d}V \tag{B.5} $$

$$ {}^t C^{A1}_{2i-1,2j} = {}^t C^{A1}_{2i,2j-1} = 0 \tag{B.6} $$

Matrix ${}^t\mathbf{C}^{A2}$ is given by

$$ {}^t\mathbf{C}^{A2} = \begin{bmatrix} & \vdots & \\ \cdots & {}^t C^{A2}_{2i-1,2j-1} \quad {}^t C^{A2}_{2i-1,2j} & \cdots \\ & {}^t C^{A2}_{2i,2j-1} \quad {}^t C^{A2}_{2i,2j} & \\ & \vdots & \end{bmatrix}_{2N\times 2N} \tag{B.7} $$

in which

$$ {}^{t}C^{A2}_{2i-1,2j-1} = \int_{{}^{t}V} {}^{t}\rho h_i h_j \sum_{k=1}^{N} \frac{\partial h_k}{\partial {}^{t}x} {}^{t}\bar{v}_{xk} {}^{t}\mathrm{d}V \tag{B.8} $$

$$ {}^{t}C^{A2}_{2i-1,2j} = \int_{{}^{t}V} {}^{t}\rho h_i h_j \sum_{k=1}^{N} \frac{\partial h_k}{\partial {}^{t}y} {}^{t}\bar{v}_{xk} {}^{t}\mathrm{d}V \tag{B.9} $$

$$ {}^{t}C^{A2}_{2i,2j-1} = \int_{{}^{t}V} {}^{t}\rho h_i h_j \sum_{k=1}^{N} \frac{\partial h_k}{\partial {}^{t}x} {}^{t}\bar{v}_{yk} {}^{t}\mathrm{d}V \tag{B.10} $$

$$ {}^{t}C^{A2}_{2i,2j} = \int_{{}^{t}V} {}^{t}\rho h_i h_j \sum_{k=1}^{N} \frac{\partial h_k}{\partial {}^{t}y} {}^{t}\bar{v}_{yk} {}^{t}\mathrm{d}V \tag{B.11} $$

Matrix ${}^{t}\mathbf{C}^{A3}$ is given by

$$ {}^{t}\mathbf{C}^{A3} = \begin{bmatrix} & \vdots & \\ \cdots & {}^{t}C^{A3}_{2i-1,2j-1} \quad {}^{t}C^{A3}_{2i-1,2j} & \cdots \\ & {}^{t}C^{A3}_{2i,2j-1} \quad {}^{t}C^{A3}_{2i,2j} & \\ & \vdots & \end{bmatrix}_{2N\times 2N} \tag{B.12} $$

in which

$$ \begin{aligned} {}^{t}C^{A3}_{2i-1,2j-1} = {}^{t}C^{A3}_{2i,2j} = \int_{{}^{t}V} {}^{t}\rho h_i \Bigg[\Bigg[& \frac{\partial h_j}{\partial {}^{t}x} \sum_{k=1}^{N} \frac{\partial h_k}{\partial {}^{t}x} \\ & \times ({}^{t}\bar{v}_{xk} - 2\,{}^{t}\bar{v}^{g}_{xk}) + \frac{\partial h_j}{\partial {}^{t}y} \sum_{k=1}^{N} \frac{\partial h_k}{\partial {}^{t}x} \\ & \times ({}^{t}\bar{v}_{yk} - 2\,{}^{t}\bar{v}^{g}_{yk}) \Bigg] \sum_{k=1}^{N} h_k ({}^{t}\bar{v}_{xk} - {}^{t}\bar{v}^{g}_{xk}) \\ & + \Bigg[\frac{\partial h_j}{\partial {}^{t}x} \sum_{k=1}^{N} \frac{\partial h_k}{\partial {}^{t}y} ({}^{t}\bar{v}_{xk} - 2\,{}^{t}\bar{v}^{g}_{xk}) \\ & + \frac{\partial h_j}{\partial {}^{t}y} \sum_{k=1}^{N} \frac{\partial h_k}{\partial {}^{t}y} \times ({}^{t}\bar{v}_{yk} - 2\,{}^{t}\bar{v}^{g}_{yk}) \Bigg] \sum_{k=1}^{N} h_k \\ & \times ({}^{t}\bar{v}_{yk} - {}^{t}v^{g}_{yk})] \Delta t \, {}^{t}\mathrm{d}V \end{aligned} \tag{B.13} $$

$$ {}^{t}C^{A3}_{2i-1,2j} = {}^{t}C^{A3}_{2i,2j-1} = 0 \tag{B.14} $$

Matrix ${}^{t}\mathbf{C}^{A4}$ is given by

$$ {}^{t}\mathbf{C}^{A4} = \begin{bmatrix} & \vdots & \\ \cdots & {}^{t}C^{A4}_{2i-1,2j-1} \quad {}^{t}C^{A4}_{2i-1,2j} & \cdots \\ & {}^{t}C^{A4}_{2i,2j-1} \quad {}^{t}C^{A4}_{2i,2j} & \\ & \vdots & \end{bmatrix}_{2N\times 2N} \tag{B.15} $$

in which

$$ \begin{aligned} {}^{t}C^{A3}_{2i-1,2j-1} = {}^{t}C^{A3}_{2i,2j} = \int_{{}^{t}V} {}^{t}\rho \Bigg[& \left(\frac{\partial h_i}{\partial {}^{t}x} \frac{\partial h_j}{\partial {}^{t}x} + h_i \frac{\partial^2 h_j}{\partial {}^{t}x^2} \right) \\ & \times \left[\sum_{k=1}^{N} \frac{\partial h_k}{\partial {}^{t}x} ({}^{t}\bar{v}_{xk} - {}^{t}\bar{v}^{g}_{xk}) \right]^2 \\ & + \left(\frac{\partial h_i}{\partial {}^{t}x} \frac{\partial h_j}{\partial {}^{t}y} + \frac{\partial h_i}{\partial {}^{t}y} \frac{\partial h_j}{\partial {}^{t}x} + 2h_i \frac{\partial^2 h_j}{\partial {}^{t}x \partial {}^{t}y} \right) \\ & \times \sum_{k=1}^{N} h_k ({}^{t}\bar{v}_{xk} - {}^{t}\bar{v}^{g}_{xk}) \sum_{k=1}^{N} h_k ({}^{t}\bar{v}_{yk} - {}^{t}\bar{v}^{g}_{yk}) \\ & + \left(\frac{\partial h_i}{\partial {}^{t}y} \frac{\partial h_j}{\partial {}^{t}y} + h_i \frac{\partial^2 h_j}{\partial {}^{t}y^2} \right) \\ & \times \left[\sum_{k=1}^{N} h_k ({}^{t}\bar{v}_{yk} - {}^{t}\bar{v}^{g}_{yk}) \right]^2 \Bigg] \Delta t \, {}^{t}\mathrm{d}V \end{aligned} \tag{B.16} $$

$$ {}^{t}C^{A4}_{2i-1,2j} = {}^{t}C^{A4}_{2i,2j-1} = 0 \tag{B.17} $$

References

1. **Bathe KJ, Ramm E, Wilson EL** (1975) Finite element formulations for large deformation dynamic analysis. Int. J. Numer. Meth. Eng. 9: 353–386
2. **Benson DJ** (1989) An efficient, accurate, simple ALE method for nonlinear finite element programs. Comput. Meth. Appl. Mech. Eng. 72: 305–350
3. **Camacho GT, Ortiz M** (1997) Adaptive Lagrangian modelling of ballistic penetration of metallic targets. Comput. Meth. Appl. Mech. Eng. 142: 269–301
4. **Haber R, Shepard MS, Abel JF, Gallagher RH, Greenberg DP** (1981) A general two-dimensional, graphical finite element preprocessor utilizing discrete transfinite mappings. Int. J. Numer. Meth. Eng. 17: 1015–1044
5. **Haber RB** (1984) A mixed Eulerian-Lagrangian displacement model for large-deformation analysis in solid mechanics. Comput. Meth. Appl. Mech. Eng. 43: 277–292
6. **Huétink J** (1982) Analysis of metal forming processes based on a combined Eulerian-Lagrangian finite element formulation. Int. Conference on Numerical Methods in Industrial Forming Processes, pp. 501–509
7. **Huétink J, Vreede PT, van der Lugt J** (1990) Progess in mixed Eulerian-Lagrangian finite element simulation of forming processes. Int. J. Numer. Meth. Eng. 30: 1441–1457
8. **Huerta A, Casadei F** (1994) New ALE applications in non-linear fast-transient solid dynamics. Eng. Comput. 11: 317–345
9. **Hughes TJR, Liu WK, Zimmermann TK** (1981) Lagrangian-Eulerian finite element formulation for incompressible viscous flows. Comput. Meth. Appl. Mech. Eng. 29: 329–349
10. **Kamoulakos A** (1990) A Simple Benchmark for Impact. Bench Mark, pp. 31–35
11. **Kennedy JM, Belytschko TB** (1981) Theory and application of a finite element method for arbitrary Lagrangian-Eulerian fluids and structures. Nuc. Eng. Des. 68: 129–146
12. **Lee EH, Mallet RL, Yang WH** (1977) Stress and deformation analysis of the metal extrusion process. Comput. Meth. Appl. Mech. Eng. 10: 339–353
13. **Liu WK, Belytschko T, Chang H** (1986) An arbitrary Lagrangian-Eulerian finite element method for path-dependent materials. Comput. Meth. Appl. Mech. Eng. 58: 227–245

14. **Liu WK, Chang H, Chen JS, Belytschko T** (1988) Arbitrary Lagrangian-Eulerian Petrov-Galerkin finite elements for nonlinear continua. Comput. Meth. Appl. Mech. Eng. 68: 259–310
15. **Prager W** (1961) Introduction to Mechanics of Continua. Ginn & Co., New York
16. **Schreurs PJG, Veldpaus FE, Brekelmans WAM** (1986) Simulation of forming processes using the arbitrary Eulerian-Lagrangian formulation. Comput. Meth. Appl. Mech. Eng. 58: 19–36
17. **Wang J, Gadala MS** (1997) Formulation and survey of ALE method in nonlinear solid mechanics. Finite Elem. Anal. Design 24: 253–269
18. **Zhu YY, Cescotto S** (1995) Unified and mixed formulation of the 4-node quadrilateral elements by assumed strain method: application to thermomechanical problems. Int. J. Numer. Meth. Eng. 38: 685–716